AD-A078 864 EG AND G INC SALEM MASS ELECTRONIC COMPONENTS DIV F/G 9/1
PLASMA CATHODE THYRATRON.(U)
SEP 79 D FLEISCHER , D TURNQUIST DAAB07-77-C-2704
UNCLASSIFIED DELET-TR-77-2704-F NL

| OF |
AD A078864

END
DATE FILMED
1-80
DDC

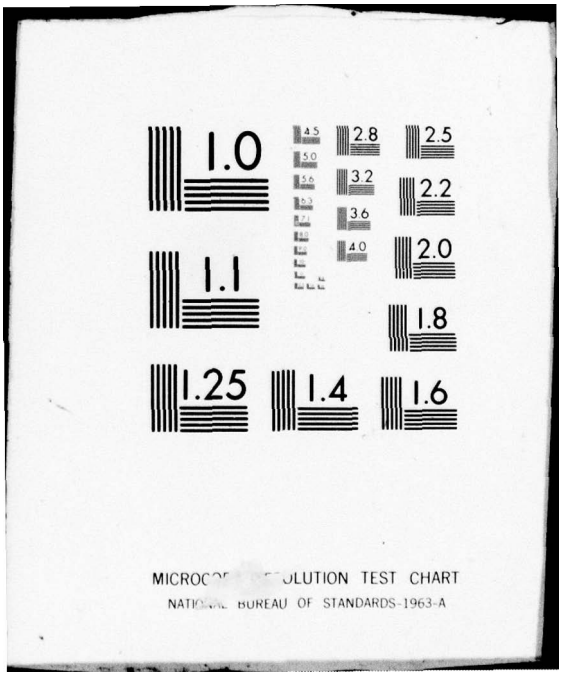
1.0
1.1
1.25
1.4
1.6
1.8
2.0
2.2
2.5
2.8
3.2
3.6
4.0
4.5
5.0
5.6
6.3
7.1
8.0
9.0
MICROCOPY RESOLUTION TEST CHART
NATIONAL BUREAU OF STANDARDS-1963-A

LEVEL II

Research and Development Technical Report
DELET-TR-77-2704-F

PLASMA CATHODE THYRATRON

David Fleischer
David Turnquist
EG&G, Inc.
Electronic Components Division
35 Congress Street
Salem, Ma. 01970

September 1979

Final Report for Period 1 September 1977 to 23 February 1979

Prepared for:
Electronics Technology & Devices Laboratory

ERADCOM
U.S. ARMY ELECTRONICS RESEARCH AND DEVELOPMENT COMMAND,
FORT MONMOUTH, NEW JERSEY 07703

NOTICES

Disclaimers

The findings in this report are not to be construed as an official Department of the Army position, unless so designated by other authorized documents.

The citation of trade names and names of manufacturers in this report is not to be construed as official Government indorsement or approval of commercial products or services referenced herein.

Disposition

Destroy this report when it is no longer needed. Do not return it to the originator.

UNCLASSIFIED

SECURITY CLASSIFICATION OF THIS PAGE (When Data Entered)

REPORT DOCUMENTATION PAGE

READ INSTRUCTIONS BEFORE COMPLETING FORM

1. REPORT NUMBER: DELET-TR-77-2704-F	2. GOVT ACCESSION NO.
3. RECIPIENT'S CATALOG NUMBER	
4. TITLE (and Subtitle): PLASMA CATHODE THYRATRON	5. TYPE OF REPORT & PERIOD COVERED: FINAL rept. 1 Sept 77 - 23 Feb 79
6. PERFORMING ORG. REPORT NUMBER	
7. AUTHOR(s): Dr. David Fleischer; Mr. David Turnquist	8. CONTRACT OR GRANT NUMBER(s): DAAB07-77-C-2704
9. PERFORMING ORGANIZATION NAME AND ADDRESS: EG&G, Inc. Electronic Components Division, 35 Congress Street, Salem, MA 01970	10. PROGRAM ELEMENT, PROJECT, TASK AREA & WORK UNIT NUMBERS: 612705. 1L1 62705 AH94 E1 10
11. CONTROLLING OFFICE NAME AND ADDRESS: US Army Electronics Technology & Devices Lab, ATTN: DELET-BG, Fort Monmouth, NJ 07703	12. REPORT DATE: September 1979
	13. NUMBER OF PAGES: 55
14. MONITORING AGENCY NAME & ADDRESS (if different from Controlling Office)	15. SECURITY CLASS. (of this report): Unclassified
	15a. DECLASSIFICATION/DOWNGRADING SCHEDULE

16. DISTRIBUTION STATEMENT (of this Report)

Approved for Public Release; Distribution Unlimited.

17. DISTRIBUTION STATEMENT (of the abstract entered in Block 20, if different from Report)

18. SUPPLEMENTARY NOTES

19. KEY WORDS (Continue on reverse side if necessary and identify by block number)

Gas Filled Device
Thyratron
Switch tube
Cold Cathode
Hydrogen thyratron

20. ABSTRACT (Continue on reverse side if necessary and identify by block number)

An instant-starting hydrogen thyratron is described which incorporates a cathode requiring no warmup time, no standby power, and no separate heater power supply. Starting cold, time jitter is less than 1 ns; anode delay time is less than 200 ns; and the 0-30 second anode delay time drift is less than 100 ns.

The cathode is a self-heating design made of impregnated tungsten. Even when cold, it provides sufficient emission capability to trigger readily and to prevent arcing. During operation, it attains full operating temperature via plasma

→over

DD FORM 1 JAN 73 1473 EDITION OF 1 NOV 65 IS OBSOLETE

UNCLASSIFIED

SECURITY CLASSIFICATION OF THIS PAGE (When Data Entered)

410 029

20. Abstract (continued)

heating effects and its own resistive dissipation; after shutdown, it remains active, in readiness for the next cold start, a cycle which can be repeated as often as desired. Thyratrons made with the new cathode display operating behavior and life comparable to conventional hydrogen thyratrons of equivalent size.

ABREVIATIONS AND SYMBOLS

Ak	cathode area
d	electrode spacing
E	plasma field
Ef	filament voltage
Eres	reservoir voltage
egy	peak open circuit grid-driver voltage
egk	grid-cathode voltage
epy	peak anode voltage
h	cathode length
Ib	average anode current
ib	peak anode current
If	filament current
ig	peak grid current
ik	peak cathode current
Ip	rms anode current, $(Ib \cdot ib)^{1/2}$
Ires	reservoir current
j	surface current density
ja	arc transition surface-current density
L	inductance
Pf	filament power
Pk	cathode discharge-heating power
pps	pulses per second
prr	pulse repetition rate
Rc	cathode internal resistance
Ro	cathode surface resistivity
T	temperature
tad	anode delay time
Δtad	anode delay-time drift

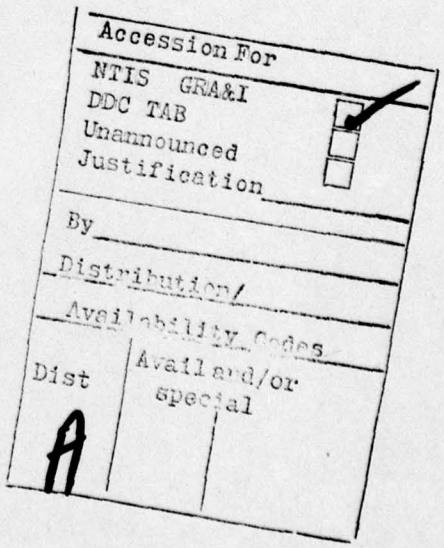

Δtas	time interval for anode delay-time drift
tj	anode time jitter
Tk	tube conditioning (preheat) time
tkp	cathode pulse width
tp	anode pulse width
tr	anode pulse rise-time
Vs	sheath voltage
W	cathode area per unit cathode length
Z	impedance
Zg	grid driver impedance
Zo	characteristic impedance

FOREWORD

This Final Report describes the work accomplished under USAECOM Contract DAAB07-77-2704, entitled "Plasma Cathode Thyratron," covering the period 1 September 1977 to 23 February 1979. This work was performed by EG&G, Inc., 35 Congress Street, Salem, Massachusetts 01970.

CONTENTS

Section		Page
	ABREVIATIONS AND SYMBOLS.	iii
	FOREWORD.	v
1.0	SUMMARY	1
2.0	PROGRAM DESCRIPTION AND RESULTS	2
	a. Introduction.	2
	b. Program Objective	2
	c. Previous Work	4
	(1) The Autron	4
	(2) Hollow Cathode Triode.	4
	(3) Grounded-Grid Thyratron.	5
	d. Technical Approach.	5
	(1) Tube Type.	5
	(2) Cathode Considerations	5
	(3) Conclusion	8
	e. Discussion of Results	8
	(1) Autron Performance	8
	(2) Discharge Heated Thyratrons.	9
3.0	DEVELOPMENT PROGRAM	16
	a. Autron Characterization	16
	(1) Tube and Circuit Configuration	16
	(2) Holdoff Voltage.	16
	(3) Time Delay and Jitter.	19
	(4) Effect of Current Ratio.	19
	(5) Conclusion	21

Section		Page
	b. Planar Impregnated Cathode Tubes.	22
	(1) Planar Cathode Triode.	22
	(2) Planar Cathode Tetrodes.	28
	c. Helical Impregnated Cathode Tetrodes.	33
	(1) Tetrode Geometry	33
	(2) Helical Cathode	35
4.0	CONCLUSIONS	43
5.0	REFERENCES	44
APPENDIX	FINAL TEST RESULTS: DHT/XPHT-1011-3203, SN 013, 014, 015.	46

LIST OF ILLUSTRATIONS

Figure		Page
1	DHT helical cathode tetrodes.	10
2	Helical cathode	11
3	Repetitive pulse test circuit	12
4	The Autron: sectional view	17
5	Autron circuit.	18
6	DHT planar cathode triode (No. 008)	23
7	Mounted planar impregnated cathode	24
8	DHT planar cathode tetrode (No. 009).	29
9	DHT helical cathode tetrode: sectional view.	34
10	Helical cathode diode voltage	39

LIST OF TABLES

Table		Page
1	Operational requirement.	3
2	DHT performance.	13
3	Autron holdoff voltage	19
4	Summary of current distribution data	21
5	Planar impregnated cathode triode performance summary.	27
6	Effect of auxiliary grid current	32
7	Helical cathode parameters	36
8	Helical cathode heat flux	41

1.0 SUMMARY

Hydrogen thyratrons that start and operate without cathode heater power have been successfully demonstrated. Operating from a cold start, with a 500 A, 1 μs pulse, at 1000 pps and 20 kV anode voltage, the tube stabilized in 1 minute to less than 1 ns anode jitter, with an anode delay time drift of 200 ns. The 265 hr life that was measured is comparable to the 250-400 hr life found with the equivalent size type 7620 hot-cathode thyratron, when life-tested under even less severe conditions. Trigger voltage and delay time at startup are decreased by means of a few milliampere, 3.7 W keep-alive discharge between an auxiliary grid and the cathode. A conventional 800 V, 6.4 W output grid driver is used, giving a power amplification factor of 500.

The ability of the tube to turn on instantly from a completely cold start, with full anode voltage, demonstrates its application to burst-mode operation. The tube utilizes a low work-function impregnated-type cathode having high cold pulse-emission capability. At cold start, discharge heating by the anode pulse quickly brings the cathode to temperature, restoring the barium monolayer on the cathode surface. Cathode heating to thermionic emission temperature is effected by interception of dissipation in the tube plasma and by cathode resistive dissipation. Upon turn-off, the activated cathode surface remains, providing the emission capability required to prevent arcing during the next cold-start operating cycle.

The program started with a literature search which led to the investigation of the Autron, a cold-cathode triode having reported operating capability in the thyratron range of interest. The reported performance of the Autron could not be confirmed.

2.0 PROGRAM DESCRIPTION AND RESULTS

a. Introduction

Program objective, selection of the technical approach, and program results are given in this section.

Developmental work and discussion of the cathode mechanism are treated in Section 3.0.

b. Program Objective

The work described herein is the first phase of a program having as a final objective a device with thyratron switching properties, capable of being instantly started, but not requiring external power for bringing either its cathode or reservoir to operating temperature.

The elimination of auxiliary power prevents the use of an electrically heated thermionic cathode. It also prevents maintaining the internal hydrogen atmosphere of the tube by means of the conventional electrically heated hydride reservoir. The parasitic reservoir, which uses heat generated by operating the tube, already provided, is in principle a nonelectrically heated reservoir suitable for steady-state pulse operation. This reservoir is presently used in commercial thyratrons[1]; also a new hydride that offered the possibility of providing the desired pressure at ambient temperature had just appeared.[2]

Use of the parasitic reservoir involves considerable development work. The reservoir must be sized in proportion to the gas clean-up rate and the thermal balance must be such that the desired tube pressure is obtained. A more extensive program would be required for the still unproven room-temperature hydride. However, these developments do represent a workable approach to a reservoir for steady-state operation, and a promising approach that is also applicable to even very short pulse bursts.

No such background of successful, or even promising, unheated cathode thyratron work existed, even after 40 years of effort.

Consequently, the program objectives considered in this work are (1) the development of a companion cathode for the above reservoir types, which also does not require heater power; and (2) its incorporation into a working thyratron.

Electrical and performance characteristic goals of this program are given in Table 1. For each of the two operating conditions, steady-state and burst-mode capability were to be demonstrated. The duty cycle for the burst mode is 60 sec on and 240 sec off.

The unusual grid-drive specifications derive from the Autron, investigation of this device being the point of departure for this program.

Table 1. Operational requirement.

Parameter	Operation I	Operation II
epy (kv)	20	20
ib (a)	500	250
tp (μs)	1	5
pps	1000	500
Grid Drive:		
egy (v)	500	500
Zg (ohm)	50	50
igy (a)	500	250
tp (μs)	2	7
tj (ns)	10	10
Δtad (ns)	500	500
Life (hr)	500	500

c. Previous Work

(1) The Autron

Three previous investigations were of special pertinence to this work. Vagin, in the Russian literature,[3] described the Autron, a triode with a cold, high work function, bare-metal cathode. His structure and electrode spacings derive from the planar electrode thyratron, but an atypical, very loosely self-baffled grid is used. Vagin's two-PFN circuit is also unusual. In addition to the anode PFN, a negative polarity cathode PFN, supplying equal current, is used. The common point of the two PFN's is the grid, which is the ground point for the triode. A cathode pulse, having a duration and current amplitude at least equal to those of the anode pulse, supposedly generates a plasma, which in conjunction with the loosely baffled grid causes this element to form a "plasma cathode," thereby preventing arcing.

Vagin's circuit condition contradicts his hypothesis that the grid acts as the true cathode. For equal currents in the two PFN's, the grid current must be zero, and the anode discharge is simply passing through the grid, as with a thyratron. Thus, the cathode for the priming discharge and that for the anode pulse are the same — the formal cathode of the triode. Despite the confused interpretation and the high trigger energy required, the Autron operating capability reported by Vagin is in the range of interest for thyratron applications.

(2) Hollow Cathode Triode

A different approach to cold cathode operation was investigated by another Russian group.[4] These triodes were reported to prevent arcing by utilizing a hollow cathode glow discharge. As with the Autron, this cathode was also a bare metal, high work-function structure.

Difficulty with long and nonreproducible delay time was experienced. Extensive cathode conditioning was only partially successful in repressing arc mode discharges. The necessity of rigorous conditioning for repressing glow-arc transitions has also been experienced with the Hughes cross-field switch tube,[5] and anomalous mode-switching has been reported in this device.[6]

(3) Grounded-Grid Thyratron

It has been demonstrated that thyratron commutation behavior can be preserved even with a cathode operating consistently in the arc mode. The grounded grid thyratron[7] utilizes the formal, hot oxide-coated cathode only as a trigger electrode. The anode pulse passes through the grid in the usual fashion, but then forms the arc cathode spot on the underside of the grid baffle; this cold, high work function element serves as the true cathode.

The low jitter of this device derives mostly from the use of the formal, hot cathode as a trigger electrode. This approach is not acceptable in the context of the present objective. Tube life, as a result of grid arc erosion and the accompanying hydrogen depletion by the sputtered metal, is much shorter than for the hot cathode thyratron.

However, the grounded-grid thyratron does show that if the cathode arc spot is confined to the cathode cavity, thyratron switching characteristics can still be had.

d. Technical Approach

(1) Tube Type

Although Vagin's explanation of the mechanism by which the Autron supposedly suppressed arcing is confusing, his data indicate that this simple cold-cathode device operated satisfactorily under conditions of practical interest for thyratron applications. Satisfactory cold cathode operation is also demonstrated by the grounded-grid thyratron, and in this case a metal vapor and hydrogen arc is the normal cathode conduction mode. For these reasons, and also because of the reported instability of the hollow cathode devices, the more conventional geometry represented by the Autron and grounded-grid tubes was chosen as the point of departure for this work.

(2) Cathode Considerations

Cold cathode thyratron operation is expected to have the following problems:

- Large tad and tj
- High grid-cathode breakdown voltage.

These parameters can be improved by maintaining a "keep-alive" priming current in the cathode cavity. However, if the current density is high enough to cause cathode arcing, additional problems are:

- Mechanical arc damage
- Hydrogen cleanup by sputtered metal
- Hold-off failure resulting from deposition of sputtered cathode material on the anode cavity wall.

Arcing is caused by the inability of the cathode to emit sufficient electrons to satisfy the circuit requirement. Discharge constriction, with the formation of a high current density cathode spot then raises the local temperature. If the temperature increased emission is still insufficient for the circuit requirement, further discharge constriction and temperature increase ultimately lead to vaporization of cathode material, and a large portion of the tube current is carried by metal ions.

The high, nonarcing current density of the hot cathode thyratron results from temperature augmented emission of its low work function surface. The dependence of thermionic emission on work function and temperature of the cathode is given by the familiar Richardson-Dushman equation.

With the pulse condition of the Operational Requirement (Table 1), and a normal 80 V grid-cathode drop, 40 W is dissipated in the cathode cavity plasma alone, and the possibility was suggested of using the tube internal losses to bring the cathode to its normal thermionic emission temperature. This "discharge heating" approach is, of itself, not novel; the oxide coated cathode can be maintained at thermionic temperature without filament power by means of a suitable pulse operating condition.

However, the oxide coated cathode is not suitable for discharge heating from a cold start. At tube start-up, the voltage gradient across the high resistance of the cold oxide layer results in arcing, thereby destroying the emission coating before the cathode can reach operating temperature.

Reliable impregnated cathodes, consisting of a tungsten matrix infiltrated with alkaline earth aluminates, have become available in recent years. The emission properties of this cathode also result from a barium monolayer, but its source of supply, barium aluminate, is contained in depth, not as a surface coating, as with the oxide cathode. The approximately ten-fold lower surface resistance[8] that results makes the impregnated cathode more suited to cold-start operation. In addition to reducing cold-start arc incidence, such an occurrence does not alter the cathode properties. Arc erosion simply uncovers a substrate of the same composition and emission capability as the original surface. During cold start, thermionic emission is negligible and the barium replacement mechanism — tungsten reduction of the aluminate followed by free barium migration to the surface — is not operative.

Thus, arc prevention as well as the desire for fast thyratron stabilization requires the time spent in cold operation to be as short as possible, and rapid attainment of high final operating temperature requires consideration of cathode thermal mass, radiation area, and conductive heat loss through the cathode mount and the surrounding gas.

Impregnated cathodes are currently used in arc-discharge flash lamps where long life and the absence of transmission reducing metal deposit on the lamp wall is required. A not unusual performance for a 0.125 diameter, 0.25 long impregnated cathode, used in an EG&G flash lamp, is:

ib = 5000 a peak	prr = 500 sec^{-1}
tp = 800 *ns*	life > 216 x 10^3 coulomb
Ib = 2 Adc average	Ip = 100 Aac rms average

The peak, average, and rms current are much in excess of the Operational Requirement (Table 1), whereas the pulse rate and total conducted charge are somewhat less.

The use of flash lamps for light generation depends on their arc-mode cathode mechanism, and the need for uniform pulse-to-pulse output requires a fixed, nonwandering cathode spot. This leads to small diameter

cathodes and very high cathode current densities, such as in the above example, and heatsinking is frequently required to prevent the electrode temperatures from becoming excessive.

In regard to discharge mode, the approximately 0.4 torr gas pressure in the thyratron results in a much more diffuse discharge than in the 400 torr flash lamp. A larger area cathode can then be used without discharge wandering induced jitter, and the more diffuse discharge will also result in a more uniform cathode temperature.

(3) Conclusion

The technical approach adopted was to investigate the Autron to see if its reported performance could be confirmed, and if the unusual grid drive used by Vagin offered any advantage over a conventional grid drive for cold cathode operation.

While this work was in progress, design and manufacture of an impregnated cathode triode with a more conventional grid was to be undertaken as the first step in investigating the properties of this type of cathode in an unheated cathode thyratron.

Both triode and tetrode designs, the latter to determine keep-alive effects, were to be considered.

e. Discussion of Results

The principal program results are given in this section. Further details and the description of the work leading to these results is given in Section 3.0, Developmental Program.

(1) Autron Performance

The point of departure for this program was an investigation of Vagin's claims for the performance of his Autron design and two PFN, grounded-grid circuit configuration.

A replica of Vagin's loosely baffled, high work function, bare metal cathode Autron was constructed and tested. It was concluded that the Autron design and pulse circuit described by Vagin did not give his reported performance, and that a more conventional thyratron geometry and grid drive, operating with a grounded cathode, offered a more promising vehicle and circuit for the development of an unheated cathode thyratron.

(2) Discharge Heated Thyratrons

A triode and several tetrodes employing impregnated cathodes that are operated without filament power were designed and tested. These tubes utilize thyratron type construction and circuitry. A conventionally baffled grid is used, and the tubes are operated in the normal grounded cathode circuit arrangement with low power thyratron type grid-drive.

Tube manufacture closely parallels standard thyratron procedures. Cathode activation during tube processing generates a low work function barium monolayer on the cathode surface. The low work function and low ohmic resistance of this surface allows a thyratron with an adequately sized cathode to be cold-started without arcing.

Proper cathode design results in rapid heating of the cathode to thermionic emission temperature by the anode pulse. During steady-state operation, the cathode temperature is also high enough that the barium monolayer is restored. This low work function surface remains when the tube is turned off, providing the emission capability for the next cold-start cycle. A switch tube employing this cathode operating mechanism is termed a "discharge heated thyratron" (DHT).

The performance, life, and operating characteristics of the DHT are given below. The experimental program which led to the development of this concept and a more complete description of the cathode and its operation are given in Section 3.0.

(a) Performance and Life

The latest tetrode design is shown in Figure 1. Aside from its helical cathode, Figure 2, the only unusual construction feature is the thermally isolated hydrogen reservoir.

DHT performance and life were determined with the repetitive pulse circuit of Figure 3, with 20 mA auxiliary grid current and about -20 V control grid bias applied to the tube. Table 2 compares tube performance with the program objectives, and with the performance of conventional tubes of the same size operated in conditions of comparable severity.

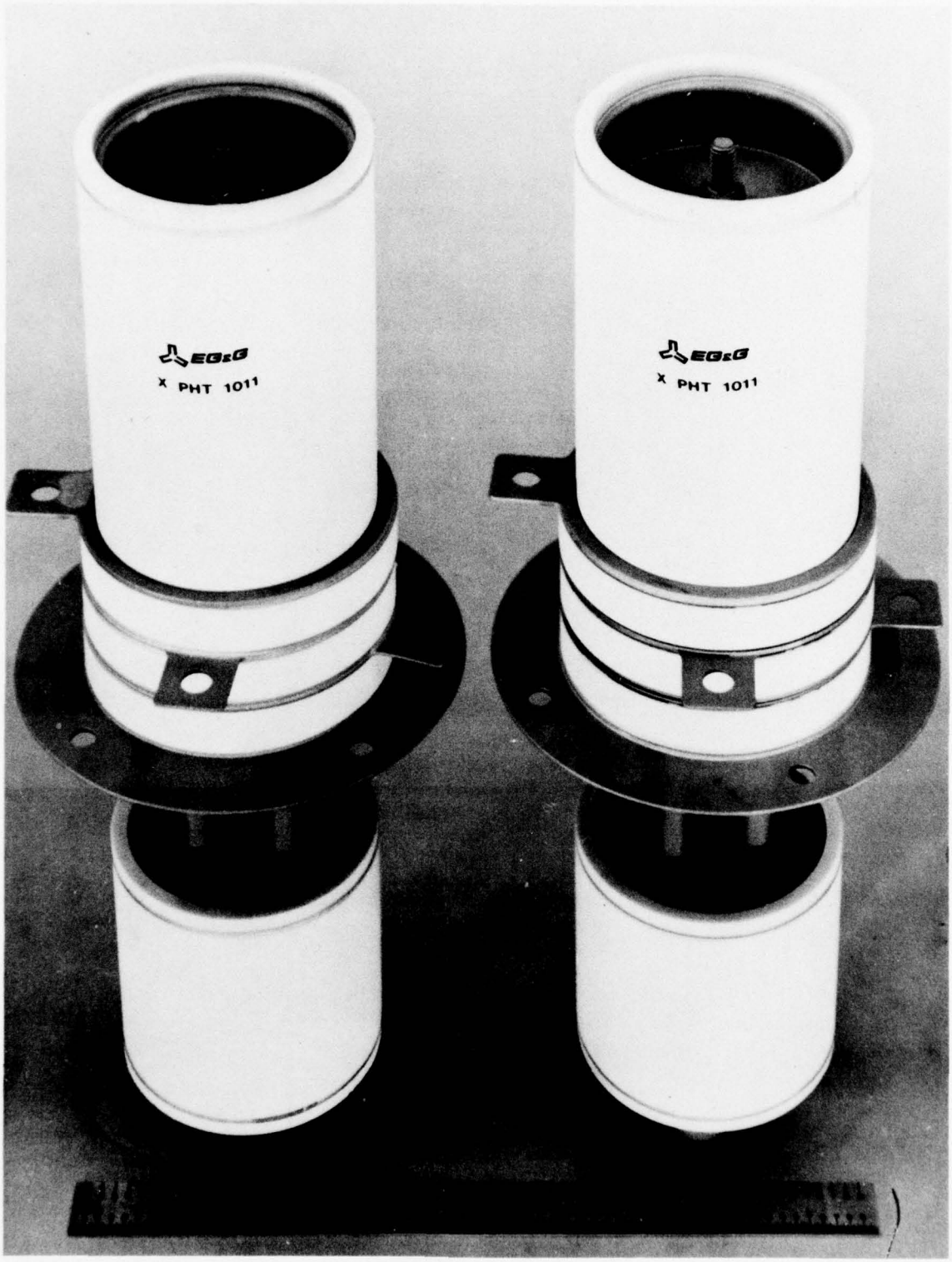

Figure 1. DHT helical cathode tetrodes.

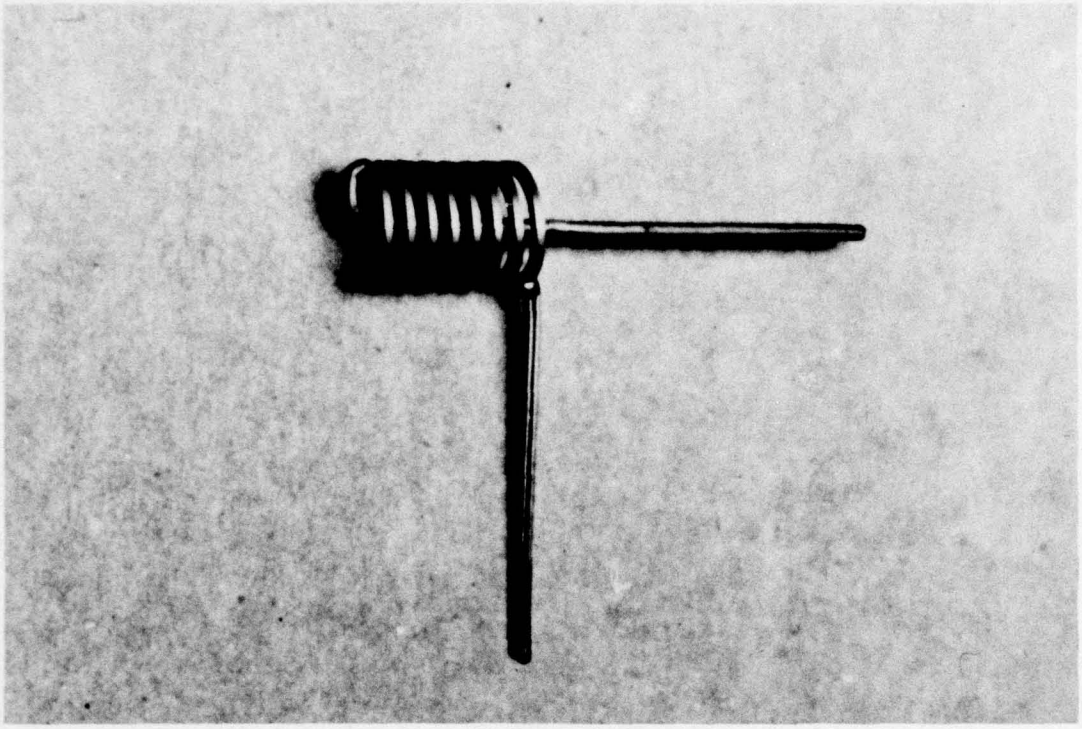

Figure 2. Helical cathode.

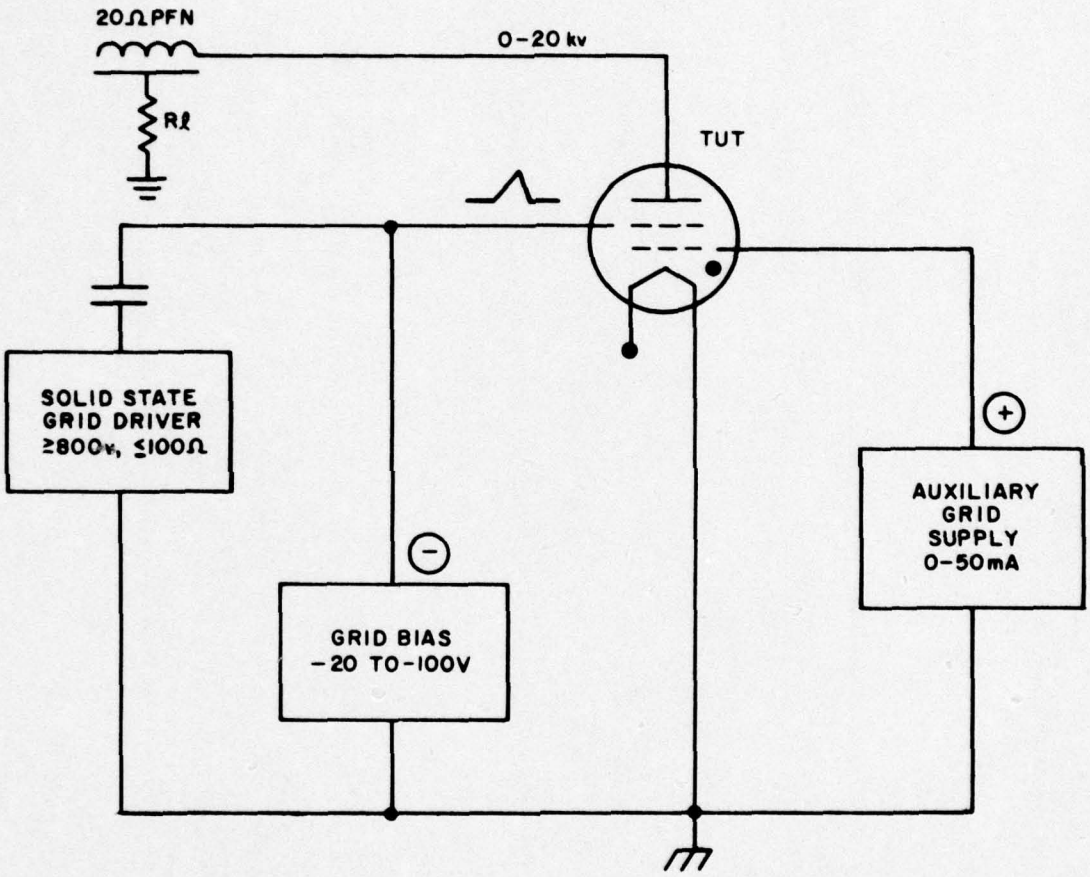

Figure 3. Repetitive pulse test circuit.

Table 2. DHT performance.

Parameter	Symbol	DHT Testing	DHT Objective	Hot Cathode 7620 Type Life Tests (Typical)	
Anode Voltage, kv	epy	20	20	20	14
Peak Current, A	ib	500	500	240	175
Pulse Width, μs	tp	1	1	1	0.42
Pulse Rate, sec^{-1}	pps	1000	1000	2000	6000
Pulse Rise-Time, ns	tr	200	NS	200	88
Average Current, Adc	Ib	0.5	0.5	0.48	0.34
RMS Current, Aac	Ip	15.8	15.8	10.7	7.2
Grid Drive:					
Control Grid Voltage, v	egy2	800	500	180	180
Control Grid Impedance, Ω	Zg2	100	50	500	500
Auxiliary Grid Current Peak, apk	igl	—	500 at 2μs tp	—	—
DC Average, ADC	Igl	0.02	1	—	—
Time Jitter, ns	tj	<1	10	<2	<1
Anode Drift:					
Drift, ns	Δtad	<100	<500	40	<50
Stabilization Time	tas	0-30 sec	NS	2-10 min	2-10
Life, hours	—	266	500	412	250-400
No. of Tubes Tested		1	—	1	5

Columns 1 and 2 of Table 2 show that the plasma cathode thyratron evaluation sample met or exceeded these objectives in all respects except life, which ended after 266 hours of operation upon failure of an internal cathode attachment weld. The truncated life does not detract from the overall significance of the development: the operating principle is successful, allowing a thyratron to be designed which meets the desired objective of a full-power start from cold.

During the life-test, the tube was cold-started a logged total of 47 times. In testing previous to being put on life, another estimated 40 to 50 cold starts were made. Repeated starting at full power from cold did not affect the triggering characteristics: time jitter remained less than 1 ns, and the 0-30 second anode delay time drift less than 100 ns.

Columns 3 and 4 of Table 2 show that conventional 2-inch tubes perform similarly under similar severe operating conditions. In the first of these test conditions, the conventional tube ran exceedingly hot and failed catastrophically. The second test produced a range of short operating life-times for the five-tube sample involved. Altogether, limited data for conventional tube operation in the vicinity of the program objectives indicate that the plasma cathode thyratron behaves much like a standard thyratron of equivalent size, and may have a somewhat similar intrinsic life.

The real differences between the DHT and hot-cathode tube are the conditioning and anode stabilization times, tk and Δtas, respectively. The typical hot cathode specification allows tk = 3 min to heat the cathode with the filament supply before turning on the thyratron. The anode drift, Δtad, is then measured over the time interval Δtas = 2-10 min after starting the tube. In the case of the DHT, the tube is cold-started, no conditioning time being required, and the very small heat capacity of the DHT cathode results in anode stabilization over the interval Δtas = 0 to about 1 minute.

(b) Burst Mode Capability

The DHT is cold-started by setting the auxiliary grid supply to 20 mA and applying 10 kV anode voltage before turning on the grid driver. The

anode PFN is resonantly charged and pulses subsequent to the first one are at the 20 kV design value. This operation was repeated about 100 times over the course of testing without the tube going into arc-initiated constant conduction. After cold starting, the DHT was repeatedly cycled off and on without any upper or lower limit being found in the length of the interburst interval.

(c) Grid Requirements

At room temperature, the grid-cathode breakdown voltage is 1.5 kV with an anode delay, tad = 1 μs. Application of a 20 mA, 185 V keep-alive discharge between the auxiliary grid and cathode reduces the trigger breakdown to 700 V, with tad = 200 ns, and this is further reduced to 400 V when the cathode comes to operating temperature. DHT tubes are currently being operated with an egy = 800 V, tp = 2 μs, zgy = 200 ohm grid driver (EG&G TM-27).

Thyratrons using keep-alive generally have a small negative bias applied to the control grid to maintain their high-voltage capability. Although no keep-alive related hold-off or recovery problems were experienced, negative grid bias was used as a precautionary measure.

3.0 DEVELOPMENT PROGRAM

a. Autron Characterization

(1) Tube and Circuit Configuration

Our copy of Vagin's Autron is shown in Figure 4. The spacings and grid dimensions were taken from Vagin's paper, the only known operational construction difference being our use of molybdenum, rather than copper, for the cathode and grid.

The features that distinguish the Autron from a thyratron are its unheated, high work function cathode and the absence of a grid baffle. Baffling depends solely on the field strength decay in the cylindrical grid apertures, which have a diameter-to-length ratio of unity. This "self-baffling" grid permits considerably more penetration of the anode field into the cathode cavity than is the case with thyratrons.

The purpose of the ceramic grid cup liner was not given by Vagin, but some such precaution, to force the grid pulse to the cathode rather than the cathode support, is necessary.

The two-PFN circuit, specified by Vagin, that was used to test the Autron is shown in Figure 5. Tube commutation is initiated by closing the mercury relay in the negatively charged cathode PFN circuit, overvolting the cathode cavity.

(2) Holdoff Voltage

The 0.080 inch anode-grid spacing of the Autron should easily be capable of withstanding 30 kV in the thyratron pressure range. The very low values actually found result from field penetration through the unbaffled grid apertures. Holdoff voltages at various internal pressures are shown in Table 3.

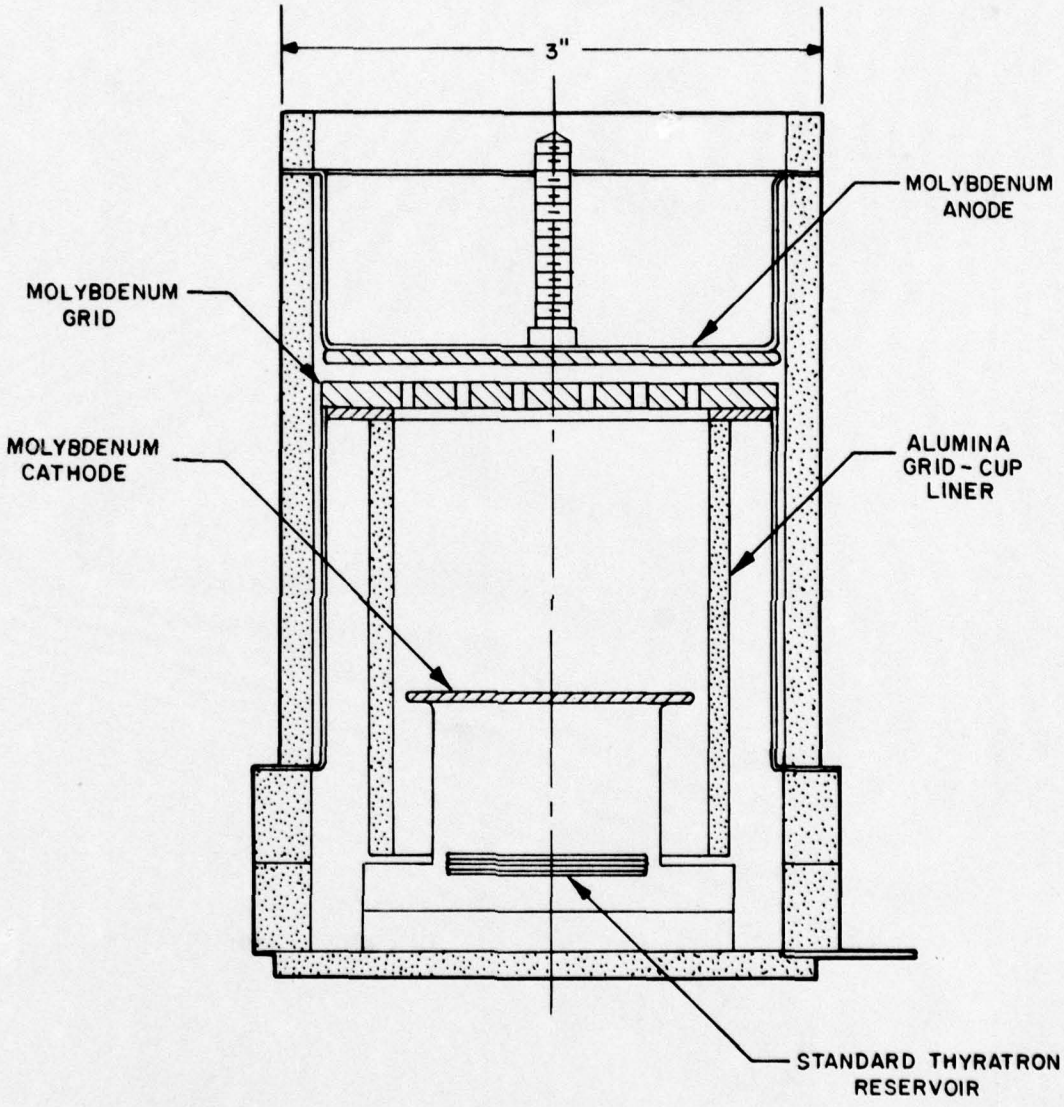

Figure 4. The Autron: sectional view.

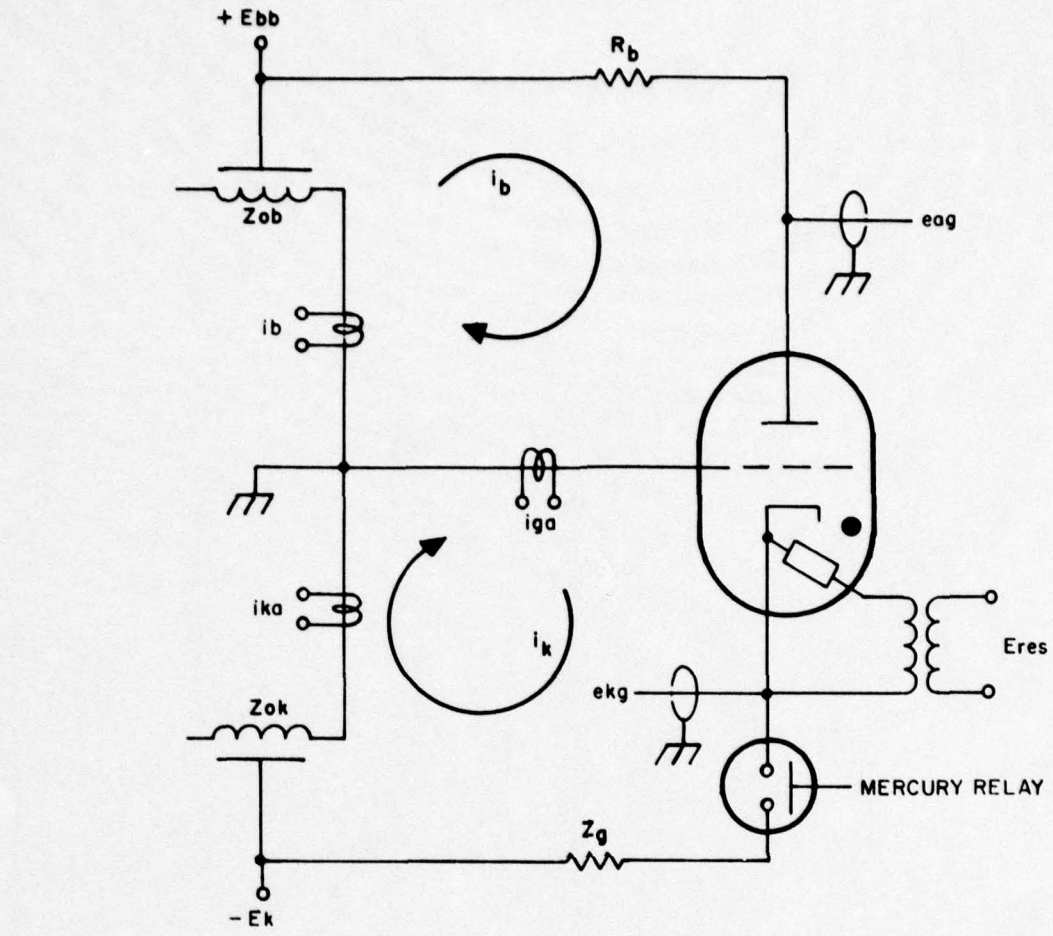

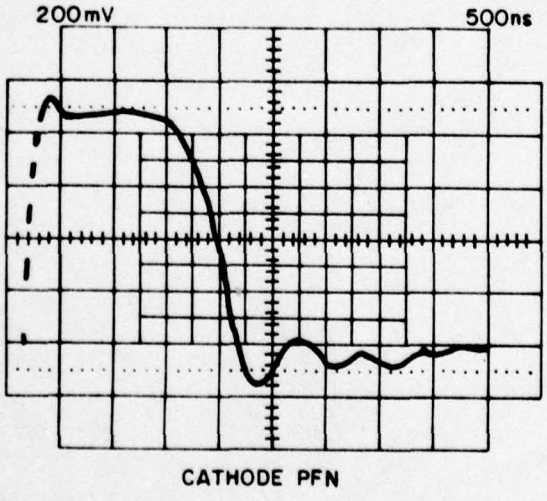

CATHODE PFN

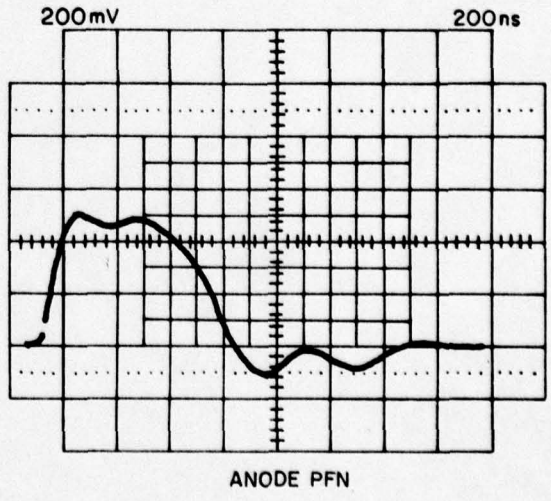

ANODE PFN

Figure 5. Autron circuit.

Table 3. Autron holdoff voltage.

Eres (Volts)	$P(D_2)$ (microns)	Holdoff (kV)
4.5	110	19.3 ± 0.7
5.6	205	18.9 ± 1.1
6.0	264	18.8 ± 0.5
6.0	300	16.0 ± 0.2
7.0	430	9.0 ± 0.4

(3) Time Delay and Jitter

The anode delay time, tad, has two components. The cathode delay, tkd, is measured from the time that the cathode voltage is applied to the time of cathode cavity breakdown. The remainder of the time required for inception of the anode pulse is the anode commutation time, tac. Whereas the anode commutation delay estimated from the data, tac $\leq$ 10 ns, is reasonable, the cathode data give an average tkd = 4.0 ± 0.5 μs for a -2.5 kV cathode voltage, which amounts to overvolting the cathode cavity by a factor of five. Lowering the voltage to -1.0 kV, and thus overvolting the cathode cavity by only a factor of two, gave such erratic results, 0 to about 15 μs, that these measurements were discontinued. These results were not affected by changing the ratio of currents in the anode and cathode loops. Such random behavior, caused by the statistical nature of the discharge time-lag and its dependence upon the ratio of the applied to static breakdown voltages, is well known.

(4) Effect of Current Ratio

The circuit of Figure 5 gives the following relationships for the cathode, anode, and grid currents:

$$ik = \frac{Zg(Ek+Ebb)+Zb\cdot Ek}{Zg(Zb+Zg)+Zb\cdot Zk} \quad (1)$$

$$ib = \frac{Zg(Ek+Ebb)+Zk\cdot Ebb}{Zg(Zb+Zg)+Zb\cdot Zk} \quad (2)$$

$$ig = ik - ib \tag{3}$$

For the load in the anode loop, as specified by Vagin, Zg = 0, and this simply reduces to:

$$ik = Ek/Zk,\ ib = Ebb/Zb,\ ig = ik - ib \tag{4}$$

In either case, three operating modes can be distinguished:

	Mode	Grid	Grid Function
(a)	ik > ib	ig > 0	anode for ik-ib
(b)	ik = ib	ig = 0	trigger electrode only
(c)	ik < ib	ig < 0	cathode for ik-ib

In modes (a) and (b), the true cathode for the anode pulse is the formal cathode of the tube, the difference being that in mode (a) the grid, in addition to serving as a trigger electrode, is also the anode for the current excess in the cathode loop. In mode (c) the grid, as well as the formal cathode, both serve as cathodes for the anode pulse.

Table 4 summarizes the current-pulse measurements over a range of cathode/anode current ratios, ik/ib. For all of these data, the anode PFN and voltage were kept constant, the variation in the cathode-to-anode current ratio and cathode pulse width (tkp) being effected by changing the voltage and number of sections of the cathode PFN. The anode current reported is its maximum value, ib, whereas the cathode and grid currents, ik and ig respectively, pertain to their values at the time corresponding to this maximum anode value. Good agreement was had between the measured grid pulse, ig, and its value calculated from the difference between the cathode and anode pulses, ik-ib. For all values of ik/ib, ranging from 0.37 to 1.2, the measured anode pulses remained constant within $\pm$4 percent.

Table 4. Summary of current distribution data.

ik/ib	tkp (μs)	Ek (kV)	ib (a)	ik (a)	ig (a)	ik-ib (a)
1.19	0.6	-2	420	500	80	80
0.76	0.4	-1	420	320	-100	-100
0.72	1.2	-1	390	280	-100	-110
0.60	0.6	-1	400	240	-140	-160
0.37	0.2	-1	405	150	-240	-255

Anode Voltage: Ebb = 5 kV

Anode Pulse Length: tp = 400 ns

The variation in Table 4 of cathode/anode current ratio from 0.4 to 1.2 should, according to Vagin, represent a transition from the arc to the "plasma cathode" mode. However, no change in anode and cathode current signals was apparent, except for ik/ib = 0.37. The anode pulse is now more noisy than for larger ik/ib, but at least some of this is a damped 45-MHz oscillation resulting from reducing the PFN to a single section.

(5) Conclusion

Our results with the Autron do not support Vagin's description of its operation. The tube design, the two-PFN, grounded-grid circuit, and the high energy driver appear to offer only operational disadvantages. The following comments are made:

(i) The self-baffled grid results in impractically low anode hold-off.

(ii) Vagin's hypothesis that the grid acts as a "plasma cathode" is in direct contradiction to his requirement that the cathode and anode PFN's carry equal currents.

(iii) If the grounded grid is forced to act as a cathode, by going to a current ratio less than unity, the Autron operates as a grounded-grid thyratron with large tad and tj.

(iv) If the current equality condition is preserved, the grid function is that of a trigger electrode only and the Autron operates as a thyratron with a cold, high work function cathode.

(v) If the current ratio is made larger than unity, the only result is to increase the cathode current density beyond that which is required for the anode pulse alone.

(vi) Excessive anode delay and jitter are had with a cold, high work function cathode.

b. Planar Impregnated Cathode Tubes

In this section, the different experimental tubes are identified by a 3-digit serial number. These numbers are sequential in terms of tube design, but not necessarily in regard to their order of investigation.

(1) Planar Cathode Triode

(a) Tube Design and Processing

A sectional view of the No. 008 impregnated cathode triode and a plan view of the grid and cathode baffle are shown in Figure 6. A planar cathode and indirect heater assembly, identical to the one shown in Figure 7 except that the surface was completely flat, was used in this tube.

Tube design follows accepted thyratron procedures. The grid assembly is provided with sufficient aperture area to ensure that quenching does not occur with the specified ib = 500 a anode pulse. The grid and grid-baffle slots are mutually parallel; this design was adopted to provide a constant lateral displacement, termed "offset" between the two sets of slots, allowing systematic adjustment of this parameter, if required. This eventuality was not realized, and the original offset and grid-baffle spacing, both typical thyratron values, were used in all of the impregnated cathode tubes.

The cathode baffle, also shown in Figure 6, is oriented to occlude any "line-of-sight" path between the cathode surface and the grid slots. This

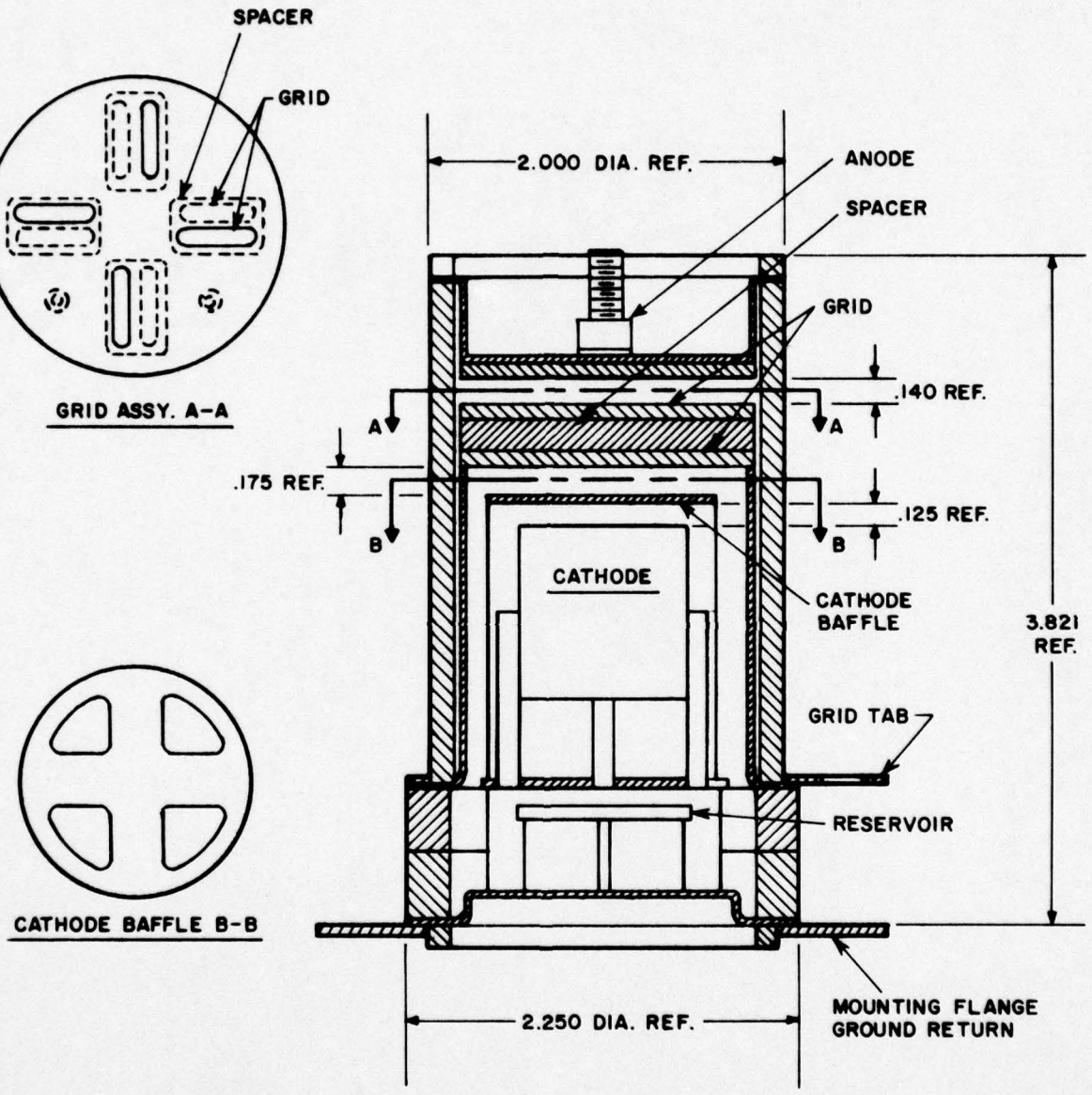

Figure 6. DHT planar cathode triode (No. 008).

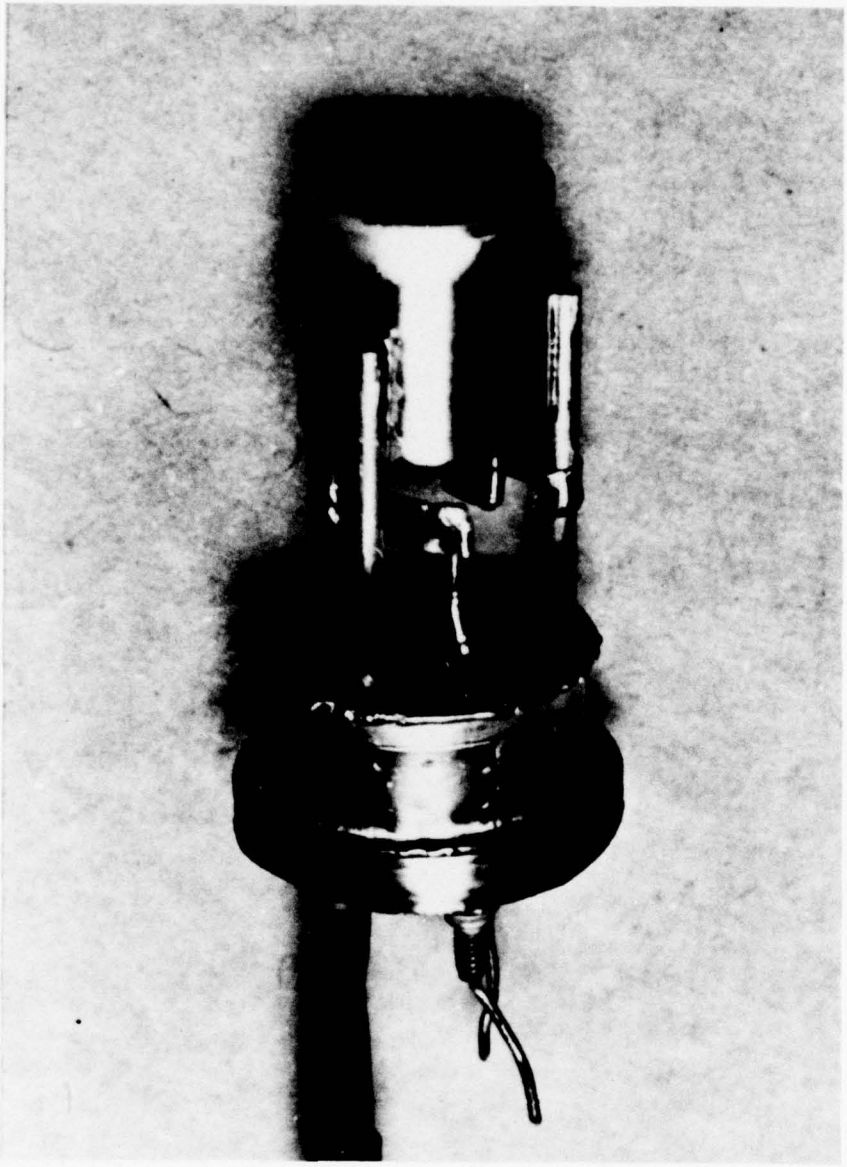

Figure 7. Mounted planar impregnated cathode.

is also accepted thyratron practice and assists in achieving high anode holdoff voltage.

Tube processing follows normal thyratron procedures. The indirect heater is used to activate the cathode and is also used when the tube is aged. The finished thyratron is thus provided with the barium monolayer on the cathode required for high emission capability.

(b) Arc Transition Current Density

The cathode area for a given pulse amplitude must be large enough that the surface current density does not reach the value at which arcing occurs. The most severe condition in discharge heated operation is at start-up, when the emission capability of the initially cold cathode is at its minimum.

To determine the cold-cathode arc-transition current density, the No. 008 tube was operated as a diode (the grid serving as the anode) over a range of pulse currents. Cathode heating was prevented by operating the diode with single, isolated pulses.

The flat surface of the cathode ensures uniform current distribution, and arcing is readily detected by step discontinuities in the oscilloscope trace of the diode voltage drop. The normal diode drop is 160 V, decreasing to 50-80 V when arcing took place.

The arc condition for the 1-inch diameter cold impregnated cathode was determined to be ja = 80 A/cm^2, arcing being evident in about one out of every ten pulses at this current density, and occurring about 200 ns after the start of the tp = 1 μs pulse.

(c) Grid-Drive Requirement

The static breakdown voltage of the No. 008 tube grid-cathode cavity at normal tube operating pressure, 400μ hydrogen, is 450 V with the cathode at room temperature. Under transient conditions, however, such as when a grid pulse is applied, higher voltage is required for reasonable cathode delay time and jitter.

Using the single pulse circuit of Figure 5, with the No. 008 triode connected as shown, tad was decreased from 3.0 to 0.8 μs by increasing egy from 1 to 5 kV with tj<50 ns throughout this range. The very considerable reduction of these parameters, in comparison to the molybdenum cathode Autron, results from the low work function of the impregnated material.

(d) Repetitive Pulse Operation

Triode No. 008 was tested under repetitive pulse conditions with the following drivers:

EG&G Driver	egy	Zg	pps (max)
Modified TM-27	175 V	500 ohm	2500
TM-30	2 kV	100 ohm	250

When the TM-27 driver was used, filament current had to be applied during start-up to decrease the grid breakdown voltage.

The test conditions and results are summarized in Table 5, where the experimental runs are listed in the order of increasing average and rms currents, Ib and Ip. These two quantities produce cathode discharge heating by dissipation in the cathode sheath and surface resistance:

$$\text{sheath dissipation} = IbVs$$
$$\text{surface resistive dissipation} = Ip^2Ro/Ak$$

It is apparent that the increasing order of Ib and Ip, and thus discharge heating, corresponds to a generally decreasing trend in tad and tj, although this correlation is partially clouded by variation in the tube internal pressure.

During the course of Runs 1-8, periodic increases in Eres were required to maintain tube operation, and during Run 8 even the maximum reservoir voltage, Eres = 8 V, was not sufficient. Inadequate fill pressure was indicated by an increased grid breakdown voltage and it was observed that this was accompanied by a partial recovery of anode voltage during pulse commutation. This latter effect was also present in low Ib and Ip runs, even when the grid signal gave no evidence of gas starvation, and thus is also indicative of low cathode temperature.

Table 5. Planar impregnated cathode triode performance summary.

Run	Mode*	Conditions						Results		
		epy (kV)	pps	tp (μs)	ib (a)	Ib (A)	Ip (A)	tad (μs)	Δtad† (ns)	tj (ns)
1	CC	4	250	1	40	0.01	0.63	2		
2	CC	10	125	1	100	0.0125	1.12	2	250	100
3	CC	10	250	1	100	0.025	1.58	1.8		
4	CC	20	250	1	200	0.05	3.2	2	500	30
5	CC	20	250	1	200	0.05	3.2	1.8		
6	FC	20	1000	1	200	0.20	6.3	0.25		<20
7	FF	20	2500	0.67	200	0.34	8.2	0.2		
8	CC	20	250	2.5	500	0.31	12.5	Commutation Failure††		
9	CC	22.5	220	2.5	900	0.50	21.2	0.1	500	<20
10	CC	25.0	220	2.5	1000	0.56	23.7	0.1	500	<20
Life	FC	20	1000		500	0.50	15.8	Life: 8 hours		
					Operational Requirement					
OPI	CC	20	1000	1	500	0.50	15.8	NS	500	10
OPII	CC	20	500	5	250	0.63	12.6	NS	500	10

* CC = cold cathode start-up and operation
FC = filament heated cathode at start-up only
FF = filament heated cathode throughout

† Δtad measured over 1-10 min running time interval

†† Caused by hydrogen cleanup

(e) Life Test

The reservoir was refilled prior to Runs 9 and 10. Following these runs, the No. 008 triode was installed in a Junior kit which had just been fitted with a PFN and load for the OPI condition of the Operational Requirement. A TM-27 driver was used for the life test. The grid unloaded after 4 hours running time and breakdown could not be reinstituted by turning on the filament supply and increasing Eres to 8 V. Considering that the Ib and Ip values of Runs 9 and 10 are equal to or larger than the OPI values (Table 5), the 4 hours elapsed during these runs were added to the life run to get the 8-hour life-time reported in the table.

The reservoir would not respond when an attempt was made to again refill it.

(f) Conclusion

The triode design essentially met the operational requirements, but with marginal triggering characteristics. Accordingly, the following measures were initiated:

(i) Design of a cathode that would have a faster thermal response and reach a higher final temperature.

(ii) Design and construction of tetrodes to determine the efficacy of keep-alive for reducing the high egy requirement, and for decreasing Δtad and tj.

(2) Planar Cathode Tetrodes

The tetrode investigation was initiated with planar cathodes already on hand. A sectional view of the No. 009 tetrode is shown in Figure 8. The No. 010 tetrode is the same, except for cathode baffling, as discussed below.

(a) Cathode Cavity Spacings

Hot cathode thyratrons sometimes utilize axial and radial spacings in the cathode cavity that would ordinarily be expected to result in long-path discharges terminating on tube elements other than the cathode. This increased design freedom results from the low work function and high emission of the hot cathode, which sufficiently decreases the breakdown voltage so that

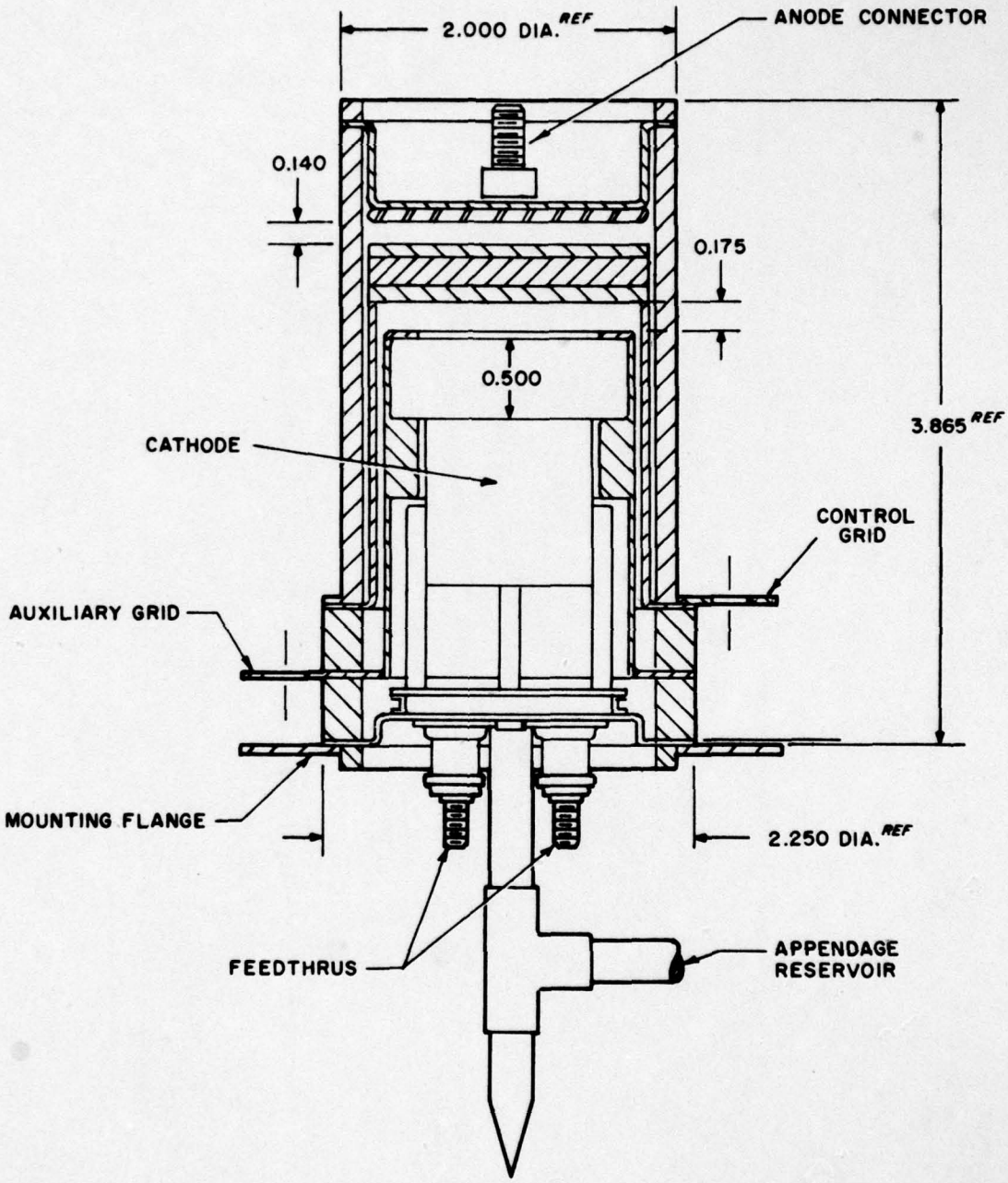

Figure 8. DHT planar cathode tetrode (No. 009).

the short-path is preferred. Although the No. 008 triode radial spacings, cathode to heat shield, and heat shield to grid cup are considerably larger than a mean-free-path, no long-path discharges occurred, indicating that even when cold, the impregnated material lowered the breakdown sufficiently that the discharge struck preferentially to the cathode.

Subsequently, tests were performed on two molybdenum cold-cathode tetrodes, No. 003 and No. 004, that had been built earlier but had never been operated. In one of these, a long-path from the auxiliary to control grid was available, and in both tubes the annulus between the auxiliary and control-grid cups was much larger than a mean-free-path. Both tetrodes exhibited long-path discharge malfunctions. A tube with a bare metal cathode is more prone to this behavior than one with an impregnated cathode, even when both are cold, but no relationship exists for permissible deviation from the long-path rule in terms of cathode activity, which in any case is not quantifiable in this context. Thus, it was not known if the proper behavior of the No. 008 triode, in spite of such deviation, was marginal or not, and it was decided in the No. 009 and No. 010 planar cathode tetrodes to rigidly adhere to axial and annular spacings that avoided long-path possibilities.

The sectional view of the No. 009 tetrode (Figure 8) illustrates the auxiliary grid support-cup design that resulted from this decision. The radial spacing between the two grid cups conforms to the mean-free-path requirement for quenching long-path discharge down the annulus. To similarly achieve this narrow spacing between the cathode and inside diameter of the auxiliary grid cup, a relatively massive filler was used. In comparison to the No. 008 triode, the increased gas conductive loss across the narrowed annulus and the much larger heat capacity of the cathode-surrounding component apparently resulted in even lower cathode temperatures in these tetrodes.

(b) Cathode Baffling

The difference in the No. 009 and No. 010 tetrodes is in their cathode baffling. The No. 009 uses a narrow, rim-like auxiliary grid, the center of which is completely open, and no baffling is interposed between the cathode and the control grid apertures.

This deletion resulted from the epy = 25 kV capability of the No. 008 triode, which suggested that tad and especially tj might be improved by a decrease in baffling without forfeiting the epy = 20 kV required by the Operational Requirement. This deviation from accepted practice proved unsuccessful; the No. 009 tetrode could be aged-up only to epy = 16 kV. To correct this, the auxiliary grid of the No. 010 tetrode had webs added across its central opening, just slightly wider than the grid slots, and this tube readily operated at epy = 20 kV, the design value. However, putting the cathode baffle on the auxiliary grid resulted in pulse-chopping. Full recovery of anode voltage is seen during the start of the pulse, followed by the final voltage drop signifying the completion of commutation.

This behavior completely disappeared when the tube was operated as a triode, with the auxiliary grid connected to the cathode. Current measurement showed the anode pulse was still going to the cathode, and not to the grounded auxiliary grid. This indicates that the observed chopping was related to the auxiliary grid voltage. This voltage floats with the control grid during commutation, and the effect is a net increase in the control grid baffling, in addition to the cathode baffling originally intended.

(c) Effect of Keep-Alive

The high voltage driver, a TM-30 modified for 1000 pps, egy = 4 kV, egz = 100 ohm, had been completed, and was used in these tests.

The performance of the No. 009 tetrode, with 20 mA keep-alive current between the auxiliary grid and cathode, is compared to that of the No. 008 triode, operating at a similar pulse condition, in Table 6.

The tad and tj improvement, in comparison to the triode values, demonstrates the efficacy of keep-alive. Three-fold and seven-fold reductions in the anode delay and jitter were found, with a reduction of anode delay drift (Δtad) by a factor of at least 50.

(d) Conclusions

(i) Keep-alive is very effective in reducing tad and tj in cold-cathode thyratrons.

(ii) Cathode baffling is needed for high voltage operation.

Table 6. Effect of auxiliary grid current.

Auxiliary Grid Current: 10 mA
Control Grid Bias: -67 V

Tube (1)	Mode (2)	epy (kV)	pps	tp (μs)	ib (a)	Ib (A)	Ip (A)	tad (ns)	Δtad (ns)	Δtas (min) (5)	tj (ns)
Tetrode	CC	16(3)	1000	1	160	0.16	5.1	90	<10(4)	0-10	3
triode	FC	20	1000	1	200	0.20	6.3	250	500	2-10	~20

Notes:

1. tetrode: tube No. 009, triode: tube No. 008.
2. CC = tube started and operated without cathode filament power
   FC = filament power at start-up only.
3. epy = 16 kV is the maximum attainable with this tube.
4. No Δtad shift, within the 20 ns resolution of the measurement, could be seen with the tetrode.
5. Δtas is the time interval over which Δtad is measured.

(iii) Cathode baffling should be at cathode potential.

(iv) The need for improved cathode thermal design is again emphasized.

c. Helical Impregnated Cathode Tetrodes

This section treats the design of a cathode and tetrode for more effective plasma heating. Four such tubes have been built; their performance has been previously described in Section 2.0, subsection e(2).

(1) Tetrode Geometry

A sectional view of the helical cathode tetrode is shown in Figure 9.

Pulse chopping induced by the effective increase in control grid baffling, when the cathode baffle voltage floats with the grid voltage, was found with the No. 010 planar cathode tetrode, as discussed in subsection b(2)(b) above. This problem is eliminated in the helical cathode tubes by restoring the cathode baffle to its usual position, on the cathode radiation shield rather than on the auxiliary grid. Examination of Figure 9 shows that the heat shield is electrically connected to the cathode, and interference with field penetration at the control grid slots does not take place.

The long-path discharge problem observed with the molybdenum cathode tetrodes (subsection b(2)(a)) and the excessive heat loss found with the close-fitting cathode radiation shield, designed to prevent this (subsection b(2)(d)) had to be reconciled. Gas conductive loss to the radiation shield was minimized by making the radial spacing between the shield and cathode as large as possible. With the 2-inch diameter tube envelope used and the 0.5-inch diameter cathode, this annulus is many free-paths wide. Long-path discharge through this space is prevented by the cathode baffle design (see Figure 9), which forces any such discharge path to first traverse the windings of the cathode. As an added precaution, the radiation shield was provided with a molybdenum foil liner, greatly reducing arc damage if such a discharge did occur. Post life-test examination of the internal parts of tube No. 012 showed that no arcing to the cathode shield had taken place.

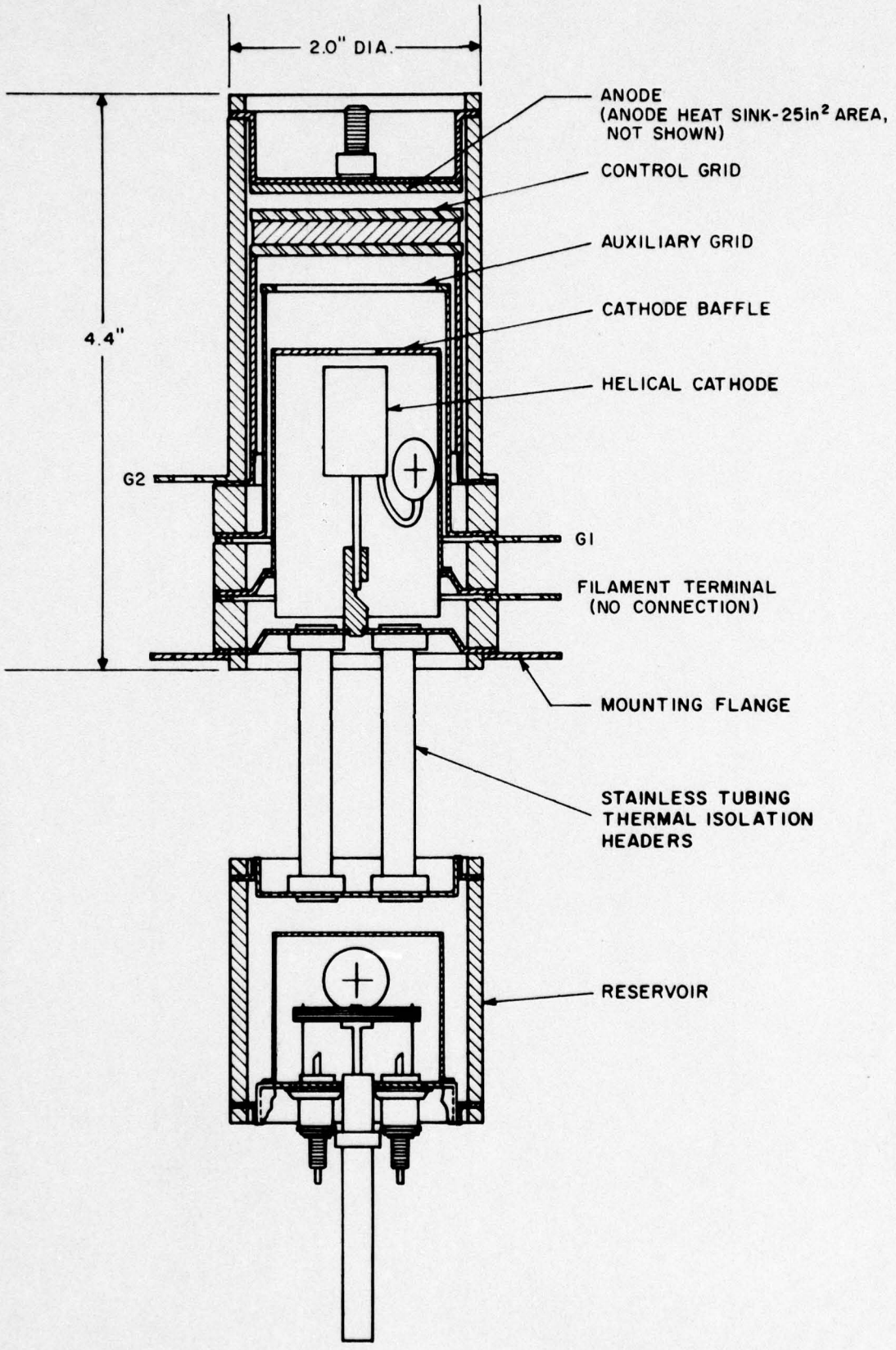

Figure 9. DHT helical cathode tetrode; sectional view.

(2) Helical Cathode

(a) Cathode Geometry

Rapid warmup and high final operating temperature require a cathode with minimum thermal mass and radiation area, with low conductive loss through the cathode mount and the surrounding gas. A large portion of the thermal mass of a cathode is contributed by its heater. This component is operationally superfluous in the DHT, but some provision for raising the cathode to temperature during its initial activation process must be made. The simplest approach is to constitute the cathode itself as a filament. A helix, mounted at its extremities, provides such a geometry. It permits electrical heating for initial activation to be done directly, and the large thermal mass of the usual indirect heater is eliminated. A helix also satisfies the low mass-to-area and low cathode-mount conductive loss requirements, and its partially self-shielding geometry is reasonable in terms of reducing radiation area and gas conductive loss.

The helical cathode used, shown in Figure 2, has the same area as the grooved indirectly heated impregnated cathode of Figure 7. The relative heat capacities of the two, 0.18 and 4.1 cal/deg, indicate the decrease in thermal mass made possible when a separate heater is not used and by an area-efficient design.

A further advantage of the filament type cathode is that it increases the discharge heating effect. In addition to the IbVs plasma term and the IP^2Ro surface resistance term, there is also an IP^2Rc contribution from the cathode internal resistance.

The particular embodiment of the filament concept that was used — the helix — does, however, have the disadvantage of being inductive. Reduced inductance was of secondary importance to the urgent need for improved cathode heating at this stage of the investigation, and the simplicity afforded by the helix took precedence over the reduced inductance cathode forms which require a more complex design.

The parameters of the helical cathode are given in Table 7.

Table 7. Helical cathode parameters.

Parameter	Symbol	Value
Length	h	1.98 cm
Diameter	—	0.5 in.
Area	Ak	12.8 cm^2
Wire Dimension	—	0.04 in. square
Internal Resistance (T=25°C)	Rc	31 m-ohm
Inductance	Lc	0.33 μH
PFN Inductance	L	10 μH

(b) Cathode Utilization

Limitation of cathode current density below the arc transition value and calculation of the discharge heating effect both depend on a knowledge of the cathode surface current distribution. The surface utilization expression for the oxide-coated vane cathode[9] is not applicable in this case, and the required utilization function, for an inductive cathode with surface and internal resistances of the same order of magnitude, was formulated too late to be fully exploited in this program. A preliminary solution of this equation indicated a progressively increasing uniformity of the surface current distribution as discharge heating increases the cathode internal resistance. Accordingly, a uniform utilization model was used for interpretive purposes in this work. The required expressions that result from this approximation are given below.

The internal current in the cathode at any point x is:

$$i(x) = W \int_x^h j\,dx \tag{5}$$

For constant j,

$$i = Wj(h-x) \tag{6}$$

and the internal resistive power dissipation is given by

$$Pc = (Wj)^2 Rc/h \int_0^h (h-x)^2 dx, \text{ and} \tag{7}$$

$$Pc = i^2 Rc/3 \tag{8}$$

where Rc is the cathode internal resistance.

Power dissipation in the cathode surface resistance is:

$$Ps = RoW \int_0^h j^2 dx = Ro \cdot i^2/Ak \tag{9}$$

An expression for the cathode voltage drop will also be required. Using Equation 6 to find the internal voltage drop, and adding on the surface resistance contribution, jRo, the voltage across the cathode is:

$$Vo = i(Rc/2 + Ro/Ak) \tag{10}$$

During the rising portion of the current pulse, an Ldi/dt inductive drop, Vq, occurs across the helical cathode. Making use of Equation 6,

$$Vq = \frac{WL}{h} \int_0^h (h-x) \frac{dj}{dt} dx \tag{11}$$

For uniform cathode utilization with a linearly rising current pulse,

$$dj/dt = ib/tr \cdot Ac \tag{12}$$

and

$$Vq = ib \cdot L/2tr \tag{13}$$

(c) Arc Transition Current

The arc condition for the cold, planar impregnated cathode was determined in subsection b(1)(b) to be 80 A/cm^2 and, assuming uniform utilization, the helical cathode was dimensioned to give an average current

density, 40 A/cm^2 for the specified ib = 500 pulse. The helical cathode was cold tested in a diode configuration, using the single pulse circuit of Figure 5. Cold cathode average current densities as high as j = 97 A/cm^2 were reached with no evidence of arcing, the pulse amplitude for this condition being the maximum for the single-pulse test circuit.

(d) Surface Resistance

The cathode surface resistance, Ro, participates in the discharge heating process and is also of interest in regard to the high arc-transition current density of the impregnated cathode. This term is customarily estimated from the variation in diode voltage drop with pulse current. [9,10]

Assuming uniform utilization, the voltage drop across the diode is given by:

$$V = (Rc/2 + Ro/Ak)ib + E \cdot d + Vs \qquad (14)$$

where the term in parentheses results from Equation 10. The plasma field, E, in Equation 14 is reasonably independent of current under hydrogen thyratron conditions[9] and the linear relationships between V and ib that are found with oxide cathodes[9,10] also indicate only minor variations in sheath voltage.

The slope of Equation 10, Rc/2 + Ro/Ak, for the cold helical cathode was determined from data taken with the single-pulse test circuit. The data, portrayed in Figure 10, indicate good linearity between V and ib over a current range of ib = 260-1240 a. Using the independently measured cathode internal resistance, Rc = 0.031 ohm, the cold cathode surface resistivity, assuming uniform utilization, is Ro = 0.11 ohm-cm^2.

(e) Discharge Heating

The total heat flux to the cathode in repetitive pulse operation, assuming uniform utilization, is estimated to be:

$$Pk = IbVs + Ip^2(Ro/Ak+Rc/3) \qquad (15)$$

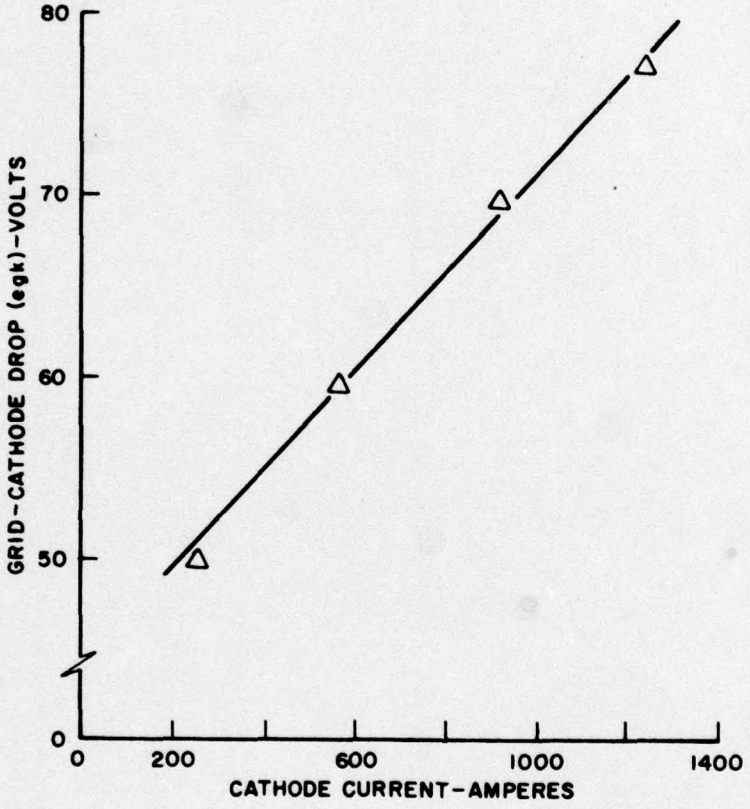

Figure 10. Helical cathode diode voltage.

The individual terms in Equation 15 are evaluated in Table 8 as a function of pulse current, where Vs = 20 V is typical of thyratron cathodes.(9)

The cathode temperatures of the first two entries in this table were found by using the helix as a resistance thermometer. The (elevated temperature:room temperature) resistance ratio of the impregnated material has been found to give temperatures, using tungsten data, that agree ±30°C with the cathode brightness temperature.(11)

Filament resistance was measured by first allowing the tube to reach thermal equilibrium under the discharge heated condition. Upon turning off the plate supply, the voltage drop across the filament, induced by a 1 ADC constant current source, is recorded against time with a digital millivolt meter. These measurements extrapolated (10 sec) to zero time give the cathode resistance, and hence temperature, at the operating condition.

The Pk column sums the individual contributions, and the Pf column is the filament power required to maintain the cathode at the same temperature in the absence of anode current. The good agreement between the heat flux given by Equation 15 and the experimental values indicate that the assumption of uniform cathode utilization is at least close enough to reality to be useful for design purposes.

The last line in Table 8 gives the calculated heat flux for the OPI condition of the Operational Requirement, and the Pk = 24 W result indicates a 650°C cathode operating temperature under these conditions.

This temperature is low for significant thermionic emission. However, the measured cathode temperatures in Table 8 are average values, giving no indication of the temperature distribution on the cathode. Equation 7 shows that the internal resistive heating increases as the square of the distance from the tip to the base of the cathode for the uniform utilization case. Thus, the temperature at the bottom of the cathode is much higher than the 650°C average. In this regard, it is interesting that post-life examination of tube No. 012 showed temperature embrittlement of the lower portion of the cathode.

Table 8. Helical cathode heat flux.

		Pulse Rate: 60 sec^{-1} Ro = 0.11 ohm-cm^2			Pulse Width: 6 μs Vs = 20 V				
ib (A)	Rc (mΩ)	T (°C)	Ib (A)	Ip (A)	IbVs	Ip^2Ro/A	$Ip^2Rc/3$	Pk	Pf
					(----------Watt----------)				
1000	117	647	0.36	19.0	7.2	3.2	14.0	25	25
1250	142	810	0.45	23.7	9.0	5.0	26.7	41	45
				OPI Condition					
500		647	0.50	15.8	10.0	2.2	11.8	24	

(f) Inductive and Temperature Effects

During the testing of the helical cathode tubes, sporadic instabilities were sometimes detected, mostly during cold-start. Grounding the cathode at the top of the helix (see Figure 9) eliminates this behavior. The improved tube performance when the cathode is grounded at the top, and the fact that no such anomalies were observed with the No. 008 triode and the No. 009 tetrode, both having planar cathodes, indicates that the inductance of the helix, not the intrinsic nature of cold cathode operation, is the cause of this behavior.

The helix, considered as a circuit element, has an inductance Lc = 330 nH, insignificant in comparison to the L = 10 μH of the OPI PFN. Although this small increment in inductance can have no effect on the anode current pulse, it can induce a comparatively large voltage drop across the cathode.

For the uniform utilization case, Equation 13 shows that the effective inductance is one-half the circuit element value, and even this 165 nH would result in an Ldi/dt = 400 v during the 200 ns rise-time of the ib = 500 a OPI pulse. This is large in comparison to the 35 V cathode resistive drop given by Equation 14 for the steady, flat-top portion of the pulse, and the tube plasma may not be able to sustain the resultant 600 V/cm field between the cathode windings.

The preliminary solution of the helix utilization problem indicates a higher than average current density at the cathode tip when the cathode is cold. This shifted distribution increases both the resistive and inductive cathode voltages and could explain the preponderance of the false triggering at start-up, decreasing later when the increase in cathode temperature equalizes the surface current distribution.

During cold-start Δtad measurements, abrupt shifts in tad are observed before it reaches its final stable value. This also is observed only with the helical, and not the planar cathode tubes, suggesting that different parts of the cathode are being used during the cathode heating period. This behavior could also be explained in terms of the predicted temperature-induced change in utilization.

(g) Life Test

Life testing was started with ib = 500 A and the pulse current reduced when hold-off failures occurred during pulse operation (nonoperating hold-off remained in excess of 20 kV to end of life). Of the 266 hour total life, 40% was accumulated at ib = 350 A. Life testing was terminated when the tube failed to trigger reliably.

Internal examination showed a broken weld joint where the cathode is attached to the ground flange. This discontinuity could explain the trigger malfunction and also, because of arcing, the random mid-life hold-off failures at ib = 500 A. No arc damage was seen on the cathode proper, grids or anode, and wall deposits were typical of those seen in hot-cathode thyratrons life tested to a normal pulse specification. The lower portion of the cathode showed high temperature embrittlement. The internal current in a filament cathode increases progressively towards the grounded end, and this damage probably resulted from excessive Ip^2Rc heating.

Externally, heavy blistering and oxidation of the anode cup indicated the excessive dissipation resulting from the pulse condition used.

4.0 CONCLUSIONS

By employing the concept of a plasma-heated cathode, it has been possible to meet the design objectives specified for an instant-start hydrogen thyratron which requires no warmup time and no heater power. Simplifying assumptions have facilitated the design of the cathode and have enabled the behavior of experimental tubes to be predicted.

Several 2-inch diameter tubes, built (other than the cathode) from standard parts, have operated consistently at the established test conditions of 20 kv anode voltage, 500 amperes peak current, 1 μs pulse width, and 1000 pps pulse repetition rate. The tubes can be turned on repeatedly when cold at full power.

Triggering requirements have been found to be less onerous than expected. With an appropriate driver and an optional keep-alive current, time jitter is less than 1 ns; anode delay time is less than 100 ns. Use of keep-alive allows the severe 0-30 second anode delay time drift requirement to be met within the 200 ns limit, with a typical measured drift of 100 ns. Use of a relatively low-powered solid state driver gives a switched power gain of 500, much higher than the minimum gain of 20 implied by the design objectives. With a high voltage driver, the tube may be operated as a triode, without keep-alive.

A representative tube accumulated 266 hours of life before failure of an internal weld prematurely terminated the life test. Indications are that the plasma-heated thyratron has an intrinsic lifetime at least comparable to standard tubes operated under similarly severe conditions.

Even in its present state of development, the tube is practical and producible. In combination with a suitable instant-start hydrogen reservoir, it will constitute a new class of high power thyratron. Able to do what arc devices cannot, it will make possible the design of new instant-start, lightweight systems.

5.0 REFERENCES

1. The parasitic reservoir is used in some English Electric Valve thyratrons, for example, the FX-2505 and FX-2517, and some EG&G thyratrons. No literature reference is known.

2. U.S. Army Research and Development Command, Fort Monmouth, New Jersey, Private communication, 1978.

3. Vagin, L.N., and Ivleva, L.G. "The Autron — a controlled plasma-cathode gas-discharge device," Pribory i Tekhnika Eksperimenta 6 157, 1968.

4. Aksenov, et al. "Controlled gas-discharge instrument with a cold hollow cathode," op. cit 4 184, 1970.

   Aksenov, et al. "Low pressure spark gap switch with hollow pilot electrode," op. cit. 6 218, 1970.

   Aksenov, et al. "Controlled gas-discharge device with cold hollow cathode," Electronic Letters 7 No. 3, 61, 1971.

   Aksenov, et al. "Some special operating features of a pulsed gas discharge device with a hollow trigger electrode," Radio Eng. and Electr. Phys. 16 No. 7, 1192, 1971.

5. Lutz. "The crossed-field switch tube," 11th Modulator Symposium, New York, New York, September 1973.

6. Harvey, R. "Crossed field closing switch development," Report DELET-TR-77-2703-F. U.S. Army Research and Development Command, Ft. Monmouth, New Jersey, 1979.

7. Turnquist, D., Merz, S. and Plante, R. "Grounded Grid Thyratrons," 12th Modulator Symposium, New York, New York, 1976.

8. Beck, A.H.W. "The institution of electrical engineers," Paper No. 2750R, 1958.

9. Goldberg, S., and Riley, D. "Research study on hydrogen thyratrons," Vol. 3, EG&G, Inc. Wellesley, Massachusetts, 1957.

10. Creedon, J.E., Schneider, S., and Cannata, F. "Cathode-grid phenomena in hydrogen thyratrons," Proc. 7th Symp. on Hydrogen Thyratrons and Modulators, Ft. Monmouth, New Jersey, 1962.

11. Cronin, J. Spectra-Mat, Inc., Watsonville, California. Private communication, 1978.

APPENDIX

FINAL TEST RESULTS:
DHT/XPHT-1011/HY-3203, S/N 013, 014, 015

Introduction

Three replicates of the successful -012 design discussed in the body of the report were manufactured as demonstration devices. They were tested at 5, 10, and 20 kV anode voltage at both 250 and 1000 pps to determine the reservoir range and the most favorable grid conditions for stable operation in the discharge heated mode. The tube configuration is shown in Figures 1 and 9.

No significant differences were seen between the three tubes.

Grid Conditions

The following conditions were found to be satisfactory for running these tubes in the discharge heated mode from a cold start, for the entirety of the above operating range.

Driver Type	egy (v)	Zg (ohm)	tp (μs)
EG&G TM-27	600	400	2 FWHM

Auxiliary Grid Current : Igl = 40 mA
Control Grid Bias: Ecc2 = -25 V

Reservoir Range

The minimum reservoir voltage was determined for both cold start and steady-state conditions. The maximum reservoir setting could be determined in only one instance. In the remainder, the maximum safe reservoir voltage was reached without the tube "kicking out." The test results, below, indicate Eres = 6.0 - 8 V as the working range. The tube fill pressure was 0.4 Torr at Eres = 6.3 Vac.

	Eres				
	Cathode at Steady-State				Cold Start
epy (kV)	20	10	15	20	20
Tube	Min		Max		Min
-013	5.7	>8	>8	7.3	5.8
-014	5.9	>8	>8	>8	6.0
-015	6.0	>8	>8	>8	6.0

Anode Stabilization

The anode time parameters, Δtad, tad, and tj are given in the following table. The unsigned Δtad values represent decreasing tad, whereas the "+" signed values indicate an increase in tad in that particular measurement interval, tas.

The positive Δtad excursions in the table result from the provisional cathode design. No attempt was made to refine this design to provide a uniform heating rate over the length of the cathode. The different temperatures (and hence emission), constantly changing during tube warm-up, may result in wandering on the cathode as the discharge adjusts itself to the most favorable distribution pattern.

		Δtad (ns)				tad (ns)	tj (ns)
	tas (min)	0-1	1-2	2-10	0-10	(at 10 min)	
Tube	epy (kV)						
-013	5	14	6	+ 3	17	363	<1
	10	16	18	53	87	253	<1
	20	144	8	+12	140	140	<1
-014	5	5	3	5	13	347	1
	10	26	6	+ 2	30	330	1
	20	160	+ 8	8	160	120	1
-015	5	18	10	8	36	394	<1
	10	14	+ 6	+ 2	6	344	1
	20	186	8	+10	184	126	1

Tube Grounding Configuration

The ends of the helical cathode are accessed at the tube mounting flange and the filament tab. The latter ground point provides more Ip^2Rc discharge heating, but also presents the maximum inductance to the anode pulse. The choice of ground point depends on the pulse rise time. With a tr = 1 μs pulse, the filament-tab ground gave a smoother voltage drop trace and the cathode has a higher emission capability as a result of its higher average temperature.

With the faster tr = 200 ns OP-I pulse condition, the much larger Ldi/dt causes an abrupt change in the cathode surface-current distribution during the transition from the wave front transient to the steady-state (Ldi/dt ≈ 0) flat-top portion of the pulse. Since this is evidenced as anode jitter, the above test results were obtained with the cathode grounded at the lower inductance mounting flange position.

DISTRIBUTION LIST

12 Defense Documentation Center
ATTN: DDC-TCA
Cameron Station (Bldg 5)
Alexandria, VA 22314

1 Defense Communications Agency
Technical Library Center
Code 205 (P.A. TOLOVI)
Washington, DC 20305

1 Office of Naval Research
Code 427
Arlington, VA 22217

1 Director
Naval Research Laboratory
ATTN: Code 2627
Washington, DC 20375

1 Commander
Naval Ocean Systems Center
ATTN: Library
San Diego, CA 92152

1 Rome Air Development Center
ATTN: Documents Library (TILD)
Griffiss AFB, NY 13441

1 Air Force Geophysics Lab/SULL
ATTN: S-29
Hanscom AFB, MA 01731

1 Hq, Air Force Systems Command
ATTN: DLCA
Andrews AFB
Washington, DC 20331

1 CDR, MIRADCOM
Redstone Scientific Info Center
ATTN: Chief, Document Section
Redstone Arsenal, AL 35809

1 Commandant
US Army Aviation Center
ATTN: ATZQ-D-MA
Fort Rucker, AL 36362

1 Director, Ballistic Missile Defense
Advanced Technology Center
ATTN: ATC-R, PO Box 1500
Huntsville, AL 35807

1 Commander
US Army Intelligence Center & School
ATTN: ATSI-CD-MD
Fort Huachuca, AZ 85613

1 Commander
HQ, Fort Huachuca
ATTN: Technical Reference Div
Fort Huachuca, AZ 85613

1 Commander
US Army Electronic Proving Ground
ATTN: STEEP-MT
Fort Huachuca, AZ 85613

1 Deputy for Science & Technology
Office, Assist Sec Army (R&D)
Washington, DC 20310

1 HQDA (DAMA-ARZ-D)/
Dr. F.D. Verderame)
Washington, DC 20310

1 Commandant
US Army Signal School
ATTN: ATSN-CTD-MS
Fort Gordon, GA 30905

2 Director of Combat Developments
US Army Armor Center
ATTN: ATZK-CD-MS
Fort Knox, KY 40121

1 CDR, Harry Diamond Laboratories
ATTN: Library
2800 Powder Mill Road
Adelphi, MD 20783

1 Director
US Army Ballistic Research Labs
ATTN: DRXBR-LB
Aberdeen Proving Ground, MD 21005

1 Harry Diamond Laboratories
Dept of Army
ATTN: DELHD-RCB (Dr. J. Nemarich)
2800 Powder Mill Road
Adelphi, MD 20783

1 Director
US Army Material Systems Analysis Acty
Vint Hill Farms Station
ATTN: DRXSY-MP
Aberdeen Proving Ground, MD 21005

1 Cdr, TARCOM
ATTN: DRDTA-RH
Warren, MI 48090

1 Cdr, AVRADCOM
ATTN: DRSAV-E
PO Box 209
St. Louis, MO 63166

1 Commander
US Army Satellite Communications Agency
Laboratory
ATTN: DRCPM-SC-3
Fort Monmouth, NJ 07703

1 Tri-Tac Office
ATTN: TT-SE
Fort Monmouth, NJ 07703

1 Cdr, US Army Avionics Lab
AVRADCOM
ATTN: DAVAA-D
Fort Monmouth, NJ 07703

1 Commander
US Army Nuclear & Chemical Agency
7500 Backlick Rd, Bldg 2073
Springfield, VA 22150

1 HQ, TCATA
Technical Information Center
ATTN: Mrs. Ruth Reynolds
Fort Hood, TX 76544

1 Commander, DARCOM
ATTN: DRCDE
5001 Eisenhower Ave
Alexandria, VA 22333

1 Director
US Army Signals Warfare Laboratory
ATTN: DELSW-OS
Vint Hill Farms Station
Warrenton, VA 22186

1 Commander
US Army Logistics Center
ATTN: ATCL-MC
Fort Lee, VA 22801

1 Director, Night Vision & Electro-
Optics Laboratory
ATTN: DELNV-D
Fort Belvoir, VA 22060

1 Cdr/Dir, Atmospheric Sciences
Laboratory
US Army Electronics R&D Command
ATTN: DELAS-SY-S
White Sands Missile Range,
NM 88002

1 Chief
Ofc of Missile Electronic Warfare
Electronic Warfare Lab, ERADCOM
White Sand Missile Range,
NM 88002

1 Chief
Intel Materiel Dev & Support Ofc
Electronic Warfare Lab, ERADCOM
Fort Meade, MD 20755

Commander
US Army Electronics R&D Command
Fort Monmouth, NJ 07703

1 DELCS-D
1 DELAS-D
1 DELSD-AS
1 DELET-DD
2 DELET-DT
3 DELET-BG
1 DELET-P
1 DELSD-L (Tech Lib)
1 DELSD-D
1 DELET-D
2 DELSD-L-S

Commander
US Army Communications R&D Command
Fort Monmouth, NJ 07703

1 DRDCO-COM-RO
1 ATFE-LO-EC

Commander
US Army Communications & Electronic
Materiel Readiness Command
Fort Monmouth, NJ 07703

1 DRSEL-PL-ST
1 DRSEL-MA-MP
1 DRSEL-PP-I-PI
1 DRSEL-PA

1 CINDAS
Purdue Industrial Research Park
2595 Yeager Road
W. Lafayette, IN 47096

1 MIT - Lincoln Laboratory
ATTN: Library (RM A-082)
PO Box 73
Lexington, MA 02173

1 NASA Scientific & Tech Info
Facility
Baltimore/Washington Intl Airport
P.O. Box 8757, MD 21240

1 National Bureau of Standards
Bldg 225, Rm A-331
ATTN: Mr. Leedy
Washington, DC 20231

1 Advisory Group on Electron Devices
201 Varick Street, 9th Floor
New York, NY 10014

1 Advisory Group on Electron Devices
ATTN: Secy, Working Group D (Lasers)
201 Varick Street
New York, NY 10014

1 TACTEC
Battelle Memorial Institute
505 King Avenue
Columbus, OH 43201

1 Metals and Ceramics Inf Center
Battelle
505 King Avenue
Columbus, OH 43201

1 Fusion Industries, Inc.
ATTN: Mr. Vernon Smith
P.O. Box 3183
Dallas, TX 75231

1 General Electric Co., HMED
ATTN: Mr. C.J. Eichenauer, Jr.
Court Street
Syracuse, NY 13201

1 RCA - MSR Division
ATTN: Mr. Duard Pruitt
Boston Landing Road
Moorestown, NJ 08057

1 Mr. Richard Verga
AFAPL/POD-1
Wright Patterson AFB
Dayton, OH 45433

1 Mr. Charles Cason
USA Missile R&D Command
ATTN: DRSMI-RRL
Redstone Arsenal, AL 35809

1 Dr. George Dezenberg
USA Missile R&D Command
ATTN: DRDMI-HS
Redstone Arsenal, AL 35809

1 Mr. J. O'Loughlin
Air Force Weapons Lab
Kirtland AFB
Albuquerque, NM 87117

1 Dr. M.F. Rose
Naval Surface Weapon Center
White Oak Lab
Silver Spring, MD 20910

1 Mr. L. Reginato
Lawrence Livermore Laboratory
P.O. Box 808
Livermore, CA 94550

1 Mr. Bobby Gray
Rome Air Development Center
Griffiss Air Force Base
Rome, NY 13441

1 Mr. A.E. Gordon
ITT Electron Tube Division
Box 100
Easton, PA 18042

1 Mr. Richard Fitch
Maxwell Laboratories, Inc.
9244 Balboa Avenue
San Diego, CA 92123

1 Mr. Gordon Simcox
Physics International
2700 Merced Street
San Leandro, CA 94577

1 Mr. John Moriarity
Raytheon Missile Division
Hartwell Road
Bedford, MA 01730

1 Mr. R.A. Gardenghi
Westinghouse Defense & Electronic
System Center
Friendship International Airport
Box 1897
Baltimore, MD 21203

1 Mr. Robert Feinberg
Avco Everett Research Lab
2385 Revere Beach Parkway
Everett, MA 02149

1 Mr. A. Wickson
Airesearch Manufacturing Co.
Division of Garrett Corp.
2525 West 190th Street
Torrance, CA 90509

1 Dr. Larry Amstutz
USA Mobility Equipment R&D Command
ATTN: DRDME-EA
Fort Belvoir, Virginia 22060

1 Dr. Ronald Gripshover
Naval Surface Weapons Center
ATTN: DE 12
Dahlgren, VA 22448

1 Mr. Henry Odom
Naval Surface Weapons Center
ATTN: DE 12
Dahlgren, VA 22448

1 Dr. S.A. Gilmore
State University of New York
Dept of Electrical Engineers
4232 Ridge Lea Road
Amherst, NY 14226

1 Dr. R. Harvey
Hughes Research Lab
Malibu Canyon Road
Malibu, CA 90265

1 Cdr, US Army Research Office
ATTN: DRXRO-IP
PO Box 12211
Research Triangle Park, NC 27709

1 Dr. M. Kristiansen
Texas Tech University
College of Engineering
P.O. Box 4439
Lubbock, TX 79409

1 Mr. L. Pleasance
Advanced Laser Group
Lawrence Livermore Laboratory
L 470
Livermore, CA 94550

1 Mr. Kennerud
Boeing Corporation
Box 3999
Seattle, Washington 98124

1 Mr. Jorge Jansen
Laser Division
Los Alamos Scientific Laboratory
Box 1663
Los Alamos, NM 87545

1 Mr. John Murray
Princeton University
Plasma Physics Lab
James Forrestal Campus,
P.O. Box 451
Princeton, NJ 08540

1 Mr. F. Welker
Rome Air Development Center
AFSC
Griffiss Air Force Base
Rome, NY 13441

1 Mr. J. Stover
Hughes Aircraft Corp.
P.O. Box 3310
Bldg 600, MSE 141
Fullerton, CA 92634

1 Cdr, US Army Research Office
ATTN: DRXRO-PH (Dr. R.J. Lontz)
P.O. Box 12211
Research Triangle Park, NJ 27709

1 W.J. Shafer Associates
ATTN: Mr. E. Locke
10 Lakeside Office Park
Wakefield, MA 01880

1 Science Application Inc.
ATTN: Mr. Ford
2028 Powers Ferry Road, Suite 260
Atlanta, GA 30339

1 Dr. E. Beckner
Sandia Laboratories
Albuquerque, NM 87115

1 COL P. Tannen
Air Force Weapons Lab
Kirtland Air Force Base
Albuquerque, NM 87117

1 Dr. C. Church
OD Army Research
Hq, Department of the Army
Room 3E 365
Washington, DC 20310

1 Mr. P. Mace
Los Alamos Scientific Lab
P.O. Box 1663
Los Alamos, NM 87545